nature reviews methods primers

https://doi.org/10.1038/s43586-024-00313-7

Primer

Check for updates

Origami engineering

Diego Misseroni[1,9], Phanisri P. Pratapa[2,9], Ke Liu[3,9], Biruta Kresling[4], Yan Chen[5], Chiara Daraio[6] & Glaucio H. Paulino[7,8]

Abstract

Origami traces its origins to an ancient art form transforming flat thin surfaces into various complex, fabulous 3D objects. Nowadays, such transformation transcends art by offering a conceptual framework for non-destructive and scale-independent abstractions for engineering applications across diverse fields with potential impact in education, science and technology. For instance, a growing number of architected materials and structures are based on origami principles, leading to unique properties that are distinct from those previously found in either natural or engineered systems. To disseminate those concepts, this Primer provides a comprehensive overview of the major principles and elements in origami engineering, including theoretical fundamentals, simulation tools, manufacturing techniques and testing protocols that require non-standard set-ups. We highlight applications involving deployable structures, metamaterials, robotics, medical devices and programmable matter to achieve functions such as vibration control, mechanical computing and shape morphing. We identify challenges for the field, including finite rigidity, panel thickness accommodation, incompatibility with regular mechanical testing devices, manufacturing of non-developable patterns, sensitivity to imperfections and identifying the relevant physics at the scale of interest. We further envision the future of origami engineering aimed at next-generation multifunctional material and structural systems.

Sections

[1]Department of Civil, Environmental and Mechanical Engineering, University of Trento, Trento, Italy. [2]Department of Civil Engineering, Indian Institute of Technology Madras, Chennai, India. [3]Department of Advanced Manufacturing and Robotics, Peking University, Beijing, China. [4]Independent Researcher, Paris, France. [5]School of Mechanical Engineering, Tianjin University, Tianjin, China. [6]Division of Engineering and Applied Science, California Institute of Technology, Pasadena, CA, USA. [7]Department of Civil and Environmental Engineering, Princeton University, Princeton, NJ, USA. [8]Princeton Materials Institute (PMI), Princeton University, Princeton, NJ, USA. [9]These authors contributed equally: Diego Misseroni, Phanisri P. Pratapa, Ke Liu. e-mail: gpaulino@princeton.edu

Introduction

Origami, the ancient art of paper folding, has proven to be a powerful concept, inspiring innovations in science, engineering and beyond. Folding can transform one geometric form to another, usually from two dimensions to three dimensions. This transformation creates new possibilities for scientists and engineers to design multifunctional machines, lightweight structures and architected materials. The ideas of folding-induced origami structures can be found in nature[1] (Fig. 1a), and in thin walled structures undergoing sudden large deformation[2,3] (Fig. 1b,c). A recent noteworthy engineering application of origami is the starshade structure, which is illustrated in Fig. 1d.

Mathematically, an origami structure is locally a 2D, discrete manifold, which is characterized by a set of creases, lines on the manifold where (sharp) folding occurs and folding angles of the creases that determine the amount of folding. The creases divide the manifold into 2D pieces, called panels. The creases can either be straight or curved lines. When all the creases are straight lines, the panels are polygonal in shape[4]. The points of intersection of the creases are referred to as the vertices. The local structure of an origami design refers to any portion of the origami that is away from boundaries and intersections of multiple panels[5]. Some origami do not have any boundaries, forming enclosed polyhedra. In the remainder of this Primer, unless otherwise stated, origami refers to patterns with straight creases and thin panels.

Depending on the direction of the folding of the crease, when folded up creases are categorized as mountain folds and when folded down they are valley folds. The mountain/valley (M/V) assignments are relative because, depending on the viewing angle, mountain folds can be viewed as valley folds, and vice versa, but they are always pointing to opposite directions (locally). Such a convention leads to the crease pattern, a blueprint for origami structures, as shown in Fig. 1e.

Developability

Following the instruction of the crease pattern, typical origami folds up from a flat sheet into a 3D shape through isometric, or nearly isometric, transformation, without subjecting the sheet to stretch or tearing. Such an origami structure, with a flat initial state, is called developable (for example, Hypar origami). Theoretically, when the thickness of the sheet is assumed to be zero, the volume encompassed by the origami structure in its developed state is zero. To determine whether an origami structure is locally developable from its crease pattern, the N panel angles (for example, $\{\alpha_i,\ i = 1 \ldots N\}$), or sector angles, meeting at a vertex can be added up. If their sum is 360° (or 2π), this vertex can be flattened onto a plane (see Fig. 1f). Mathematically, this condition is expressed as:

$$\alpha_1 + \alpha_2 + \alpha_3 + \ldots + \alpha_N = 2\pi \tag{1}$$

If all vertices of an origami structure are developable, this origami is globally developable. This rule only applies to vertices with neighbourhoods that are locally 2D manifold.

Flat foldability

When the folding-induced transformation includes a state (other than the developed state) in which the entire origami structure can be flattened onto a plane, typically with overlapping of panels, the corresponding origami is called flat-foldable (for example, the Kresling tube). Flat foldability is a new, independent property from developability, for example, the eggbox is not developable but flat-foldable. The folded planar state is referred to as the flat-folded state. In general, there may be more than one flat-folded state for an origami structure. The Kawasaki–Justin theorem gives the necessary and sufficient conditions locally for an origami vertex to be flat-foldable. For an origami vertex with N consecutive panel angles (N must be even) labelled from 1 to N (Fig. 1g), then the vertex can be flat-foldable if:

$$\alpha_1 - \alpha_2 + \alpha_3 - \alpha_4 \ldots - \alpha_N = 0 \tag{2}$$

The variable N is called the degree of a vertex, defined as the number of creases incident on a vertex. The Kawasaki–Justin theorem deals with the panel angles but does not guide how an origami vertex can be folded flat, which relates to the M/V assignment (see Fig. 1h). The condition about fold directions for a flat-foldable vertex is the Maekawa–Justin theorem – if an origami vertex is flat-foldable, then:

$$M - V = \pm 2 \tag{3}$$

The Maekawa–Justin theorem is a locally necessary but not sufficient condition; for a crease pattern to be globally flat-foldable, all its vertices must be locally flat-foldable, which is a necessary but not sufficient condition. Any flat-foldable vertex must have even degrees (precondition of the Kawasaki–Justin theorem), which leads to a necessary criterion for global flat foldability: the two-colourability of a crease pattern (see Fig. 1e). A graph with all even degree vertices can be called a Eulerian graph, and it has been proven that Eulerian graphs satisfy two-face colouring[6]. However, flat foldability is hard[7]. The readers are referred to refs. 7,8 for more details.

Rigid foldability

During the folding-induced transformation, if the deformation of the sheet is only concentrated along the creases, without bending or stretching the panels, it is referred to as rigid origami. Such origami structure can be folded while keeping all regions of the paper flat and all crease lines straight[6]. Analysis of rigid foldability is of interest because of the increasing use of new materials other than paper for origami applications. Whereas paper is quite forgiving if the panels must deform, other materials such as metal, wood and stiff plastics are not. The well-known Miura-ori pattern, eggbox pattern, waterbomb pattern and Yoshimura pattern are all rigid origami, but the square twist[9,10] and hypar[11] patterns are not rigid origami.

A condition for rigid foldability given a single origami vertex[12,13] specifies that the product of rotation matrices about all the creases (say N in number) of a vertex should be the identity matrix ($\mathbf{I}$)[14,15], for any kinematically admissible configurations, using the Belcastro–Hull theorem:

$$\prod_{i=1}^{N} \mathbf{R}_\rho(\rho_i)\mathbf{Q}_\alpha(\alpha_i) = \mathbf{I} \tag{4}$$

where $\mathbf{R}_\rho$ and $\mathbf{Q}_\alpha$ are the transformation matrices in terms of the turning angles ρ_i and panel angles α_i, respectively (see Fig. 1i). These matrices are given by:

$$\mathbf{R}_\rho(\rho_i) = \begin{bmatrix} 1 & 0 & 0 \\ 0 & \cos\rho_i & -\sin\rho_i \\ 0 & \sin\rho_i & \cos\rho_i \end{bmatrix},\ \mathbf{Q}_\alpha(\alpha_i) = \begin{bmatrix} \cos\alpha_i & -\sin\alpha_i & 0 \\ \sin\alpha_i & \cos\alpha_i & 0 \\ 0 & 0 & 1 \end{bmatrix} \tag{5}$$

The degree-four vertex shown in Fig. 1i can be used as an example; here, $N = 4$ and when $\alpha_1 = \alpha_4 = 60°$ and $\alpha_2 = \alpha_3 = 120°$ for a particular partially folded state, the turning angles are $\rho_1 \approx -53.13°$, $\rho_2 = \rho_4 = 90°$

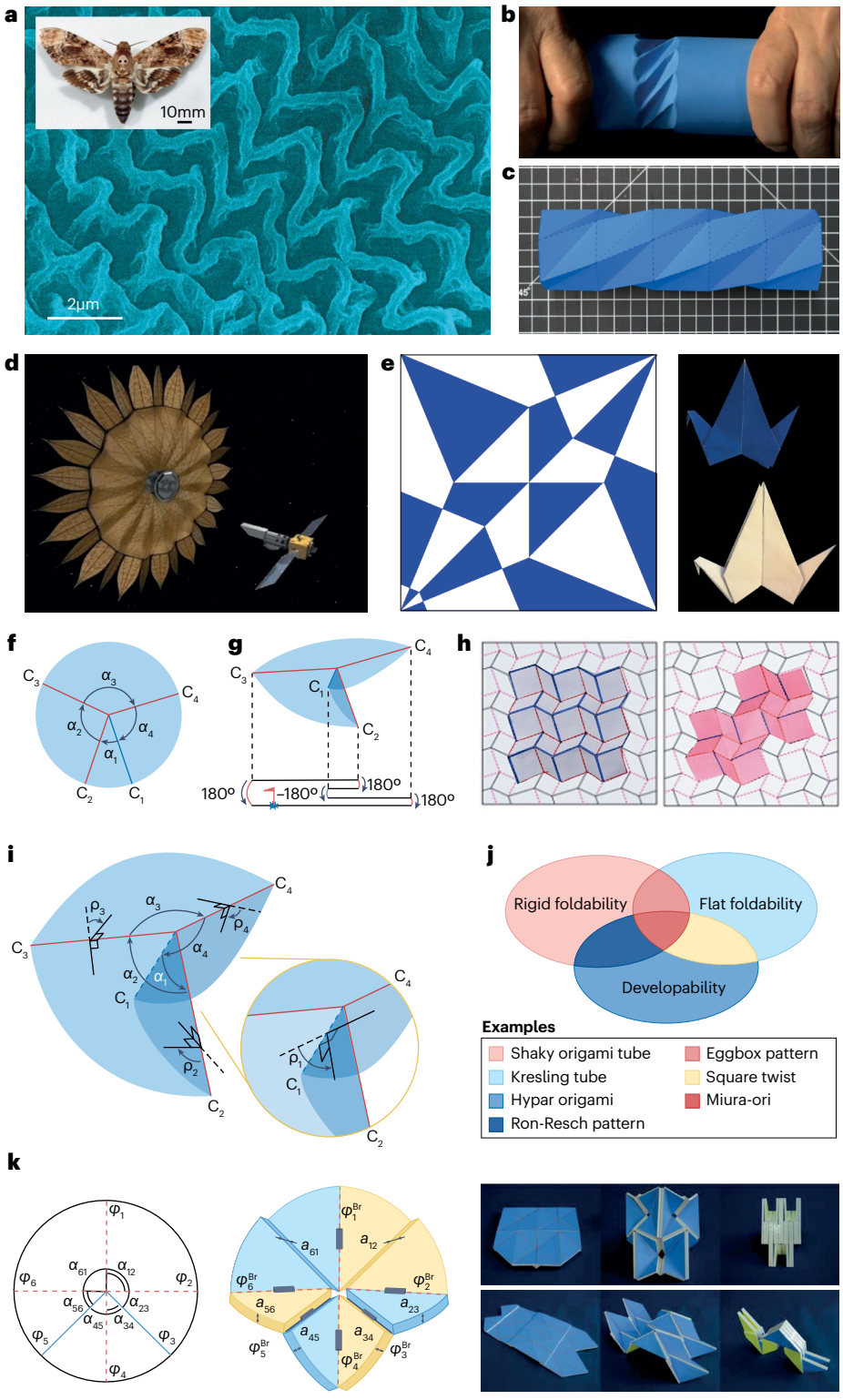

Fig. 1 | Origami overview. a, Nature-inspired origami: microscopic bellows pattern of the Giant Hawkmoth *Acherontia atropos* shown in the inset[1]. **b**, Spontaneous Kresling pattern obtained by twist buckling experiment. **c**, Kresling pattern. **d**, Unfolding of a starshade origami. **e**, Crease pattern (left) of a crane (right) using the two-colourability (colouring) property. **f**, A typical degree-four origami vertex in its developed state. **g**, Folded shape of a degree-four vertex (below: flat foldability condition). **h**, Single crease layout with a different mountain (thick continuous blue lines) and valley (thin dashed red lines): square twist (left panel) and Mars (right panel). **i**, Turning angles between the panels of a degree-four vertex used to apply the rigid foldability condition from the Belcastro–Hull condition. **j**, Venn diagram showing the relationship between flat foldability, developability and rigid foldability (left), with typical examples given (below). For a more complete list of patterns and their properties, please refer to Table 1. **k**, Thick origami models. Thickness accommodation of a waterbomb origami pattern using the offset hinge technique[17]. α_i, panel angles; φ_i, crease angles; Br, Bricard linkages; C_i, i-th crease; ρ_i, turning angles. Part **a**, image courtesy of L. T. Wasserthal. Part **d**, image courtesy of NASA/JPL. Part **k** reprinted with permission from ref. 17, AAAS.

and $\rho_3 \approx 53.13°$. The sign of the turning angle is obtained using the right-hand thumb rule with the thumb pointing along each of the creases in a consistent direction (either inward or outward from the vertex) as the fingers curl along the arrows marked for ρ_i, as shown in Fig. 1i. If the direction of the thumb must change to follow the arrow marked for a turning angle, then this suggests a change of sign. From these choices of angles, it can be shown that the product of the rotation matrices about all four creases would be an identity matrix.

Table 1 | A sample of origami patterns with featured properties, and applications

Pattern	Featured properties[a]	Engineering applications
Miura-ori	1 DOF, developability, rigid foldability, flat foldability, auxeticity	Space structures[72], metamaterials[30], frequency-selective surfaces[170], robotics[171]
Blockfold	1 DOF, developability, rigid foldability, flat foldability, auxeticity	Foldcore[83]
Eggbox	1 DOF, rigid foldability, flat foldability	Sandwich structures[172], metamaterials[30]
Waterbomb	Developability, rigid foldability, flat foldability	Smart materials[173], robotics (origami wheel)[117,174], origami stents[175]
Yoshimura	Developability, rigid foldability, flat foldability	Folded concrete structures[168]
Kresling tube	Flat foldability, multistability	Robotics[34,46], impact mitigation[176]
Morph	1 DOF, rigid foldability, flat foldability, reversible auxeticity	Metamaterials[31,121]
Barreto–Mars	1 DOF, developability, rigid foldability, flat foldability, auxeticity	Solar cells[177]
Flasher	1 DOF, developability, auxeticity	Solar sails[178]
Ron-Resch	Developability, rigid foldability	Energy absorption[179]
Miura-ori-based tubes	1 DOF, rigid foldability, flat foldability	Robotics[41]
Square twist	Developability, flat foldability, auxeticity, multistability	Metamaterials[9], programmable antennas[10]
Hypar origami	Developability, multistability	Metamaterials[4]
Origami snapology	Rigid foldability	Metamaterials[180], wave guide[181]
Trimorph	1 DOF, rigid foldability, flat foldability, reversible auxeticity, multistability	Metamaterials[32]

This is not an exhaustive list. DOF, degree of freedom. [a]Incomplete list.

The matrix approach is quite practical and useful when analysing origami structures with several vertices and creases, as the implementation can be naturally carried out using a computer program. This is typically done by modelling origami using Denavit–Hartenberg-based analysis[16] that is widely used in the analysis of linkages. The connection between linkages and origami is very useful, especially for thick origami[17,18].

To ensure both sufficiency and necessity for rigid foldability, other detailed conditions (in addition to the Belcastro–Hull theorem[12,13]) must be carefully checked, such as the bird's feet condition on *M*/*V* assignment[19], which is both necessary and sufficient for a single vertex. Based on the rank deficiency of the kinematic Jacobian matrix (a linear expansion of the Belcastro–Hull theorem), a counting rule to calculate the generic degrees of freedom (DOFs) of a finite origami pattern has been developed[14]. When the generic DOF is greater than zero, the corresponding pattern is rigidly foldable; otherwise, no decisive conclusion can be drawn. The counting rule is given as follows[14]:

$$N_{\mathrm{GDOF}} = N_{\mathrm{EO}} - 3 - \sum_{k>3} (k-3) N_{Pk} \tag{6}$$

where N_{GDOF} denotes the generic number of DOFs, N_{EO} denotes the number of boundary edges of a pattern, k is the number of sides of a polygonal panel and N_{Pk} denotes the number of k-sided polygons in an origami pattern. Based on the kinematic Jacobian matrix, a pattern with only triangular panels is guaranteed to be rigidly foldable if it has more than three boundaries[7]. However, this condition is too strict practically. For example, many degree-four origami patterns (patterns with only degree-four vertices) are rigidly foldable, but they cannot be determined by this formula and require case by case discussion[20,21]. The panel angles and *M*/*V* assignment are both critical for rigid foldability (Fig. 1h). Some ways to predict the folding behaviour of rigid origami are to use mathematical tools such as spherical trigonometry[4] or computational origami simulations[22].

It is important to realize that flat foldability, developability and rigid foldability are independent features of origami; having one feature does not imply the other (Table 1 and Fig. 1j). Different features are suited for particular engineering applications. For example, robotic actuation requires a quick deployment of motion and release of energy, and hence non-rigid origami with multistability is often exploited for those purposes. On the other hand, sandwich composite cores require mass production and high stiffness, and hence developable rigid origami patterns are often used.

Thick origami models

Origami patterns are commonly crafted from thin sheets (approaching zero thickness). To apply them to real engineering applications, thickness accommodation imposes additional constraints. In general, thick origami is treated on a case by case basis, and thus many methods exist to accommodate panel thickness[23]. By modelling thick origami using spherical linkages[18], the folding creases remain unchanged and the panels are either tapered[24] or offset[25] for compact folding with least physical interference of panels. A kinematic approach has been proposed for rigid origami of thick panels, involving the replacement of spherical linkages with spatial linkages at origami vertices consisting of four, five and six creases[17]. This is a comprehensive approach, which is capable of reproducing motions kinematically equivalent to those of zero-thickness origami (Fig. 1k). Meanwhile, to achieve the thick-panel folding of the non-developable vertex, auxiliary panels as intermediate links can be introduced to construct a plane-symmetric spatial linkage, which delivers compact folding[26]. Alternatively, a parallel-crease method can be used to create space for the panel thickness[27]; however, this method introduces extra DOFs as a four-crease vertex is transferred into an eight-bar linkage with at least two DOFs. A recent contribution to the thick-panel origami consists of applying kirigami to the thick panels, whose advantage is to obtain the most compact folding of the Miura-ori patterns with uniform thickness[28]. Additional work has been done on the physical forms of crease lines, such as rolling-contact joints[29] or compliant joints, which results in the variable kinematic models for the folding process. As there are many methods to treat thick-panel origami, it is difficult to determine which is the most efficient method without considering the practical case of interest. For example, for large-scale deployable structures, the folding ratio and the stiffness take the highest priority, whereas for micro-scale structures, the fabrication and flexibility take the main role. Hence, other methods are expected in future developments.

From an engineering perspective, a few representative origami patterns are considered in this Primer, including the Miura-ori pattern, the eggbox pattern, the waterbomb pattern and the Kresling tube.

These representative patterns are used as examples for origami experiments and manufacturing with desired rigid or non-rigid behaviour (see Experimentation). In the Results section, geometric descriptions of origami structures are provided using these patterns, and their geometric mechanics features are discussed. The unusual properties of origami structures have enabled engineering applications across different fields and scales, including sustainable and resilient buildings, mechanical metamaterials, robotics and medical devices. Furthermore, basic information for testing origami and standard formats to share origami designs are recommended. The limitations and opportunities in the context of design and manufacturing of origami, and an outlook for the future of origami in engineering are envisioned.

Experimentation

This section presents experimental equipment and manufacturing techniques to create and test origami patterns. These patterns display a range of properties, including a tunable Poisson's ratio[30,31], multistability[32–36], tunable stiffness[37–40] and others, such as shape morphing[41–43] and acoustics[44,45]. The experimental evidence of such properties requires careful sample manufacturing and the design of ad-hoc experimental set-ups. These set-ups are particularly important as the samples undergo large deformations simultaneously in longitudinal and transverse directions, owing to their intrinsic non-linear folding mechanisms. Different laboratory equipment is required depending on the type of experiment to be performed, for example, qualitative or quantitative. In the latter case, loading frames, prototyping machines, cameras, transducers and acquisition systems are needed to simultaneously test origami patterns and to record experimental data.

Manufacturing methods

Origami tessellations have a long history[7]. They can be realized by different manufacturing techniques and base materials. Some of the most common materials and techniques are addressed below.

Paper and polymer-based models. The simplest way to create origami patterns is by folding craft paper (for example, Mi-Teintes, Canson), cardboard, polyester film (for example, Grafix Drafting Film) or composite film (for example, Durilla Durable Premium Ice Card Stock)[38,46–48]. The folding lines can be marked or perforated with evenly spaced cuts. Laser cutters are used to perforate thin flat sheets along the folding lines, as shown in Fig. 2a. Other electronic cutting machines (for example, Silhouette CAMEO, Silhouette America) can also be used to perforate thin sheets that can be folded using origami principles. The main advantage of paper-based origami is its ease of realization. Furthermore, craft paper sheets have a very small thickness, thus preventing panel thickness accommodation issues when extreme folding is achieved. Although very effective, this method can induce some difficulties in quantitative testing as the paper-based panels are very flexible. In fact, out-of-plane deformation may not only be localized on the creases but also in the panels through flexural deformation. This could lead to difficulty in the experimental validation of the underlying theory as the hypothesis of rigid foldability may no longer hold.

Computer numerical control milled models. A more effective method to create origami samples suitable for mechanical testing consists of assembling base components such as unit cell strips, panels and hinges, which are cut by a computer numerical control milling machine (such as the Roland MDX 540)[49], as shown in Fig. 2b. The working principle of the milling machine concerns material removal through a rotating cutting tool driven by computer-aided design/computer-aided manufacturing (CAD/CAM) software. The base components can be made from different materials, such as polymeric (polycarbonate, polypropylene) or metallic (thin aluminium or steel sheets) materials. The main advantage of this manufacturing method is its versatility and precision, which permits the realization of complicated shapes and multistable origami tessellations. In particular, this method allows fine-tuning of the energy landscape together with the mechanical properties of the tessellation, by varying the crease thickness, panel geometry and base material[32]. An attractive material to create zero-energy creases (free-rotating hinges) is polypropylene as it guarantees excellent folding performance and fatigue resistance. On the other hand, if creases with specific rotational stiffness are required, these can be achieved by means of solid rubber (for example, silicon rubber)[32].

3D printed models. Recent developments in additive manufacturing technologies have enabled the construction of intricate and complex topologies at different scale levels[50]. In this context, 3D printing represents an alternative method to creating origami samples, as shown in Fig. 2c. The origami models are built layer by layer from a previously prepared 3D CAD file. Various materials and 3D printing technologies can be used depending on specific needs. For instance, origami tessellations have been realized by fused filament fabrication[51,52], material jetting[53], selective laser sintering[54], stereolithography[5,55], digital light processing[56,57] and, at the micro-scale, by two-photon polymerization laser lithography[58]. In addition, 4D printing adds the transformation over time (fourth dimension) to 3D printing, which has been used to create multifunctional shape-morphing and self-foldable origami-based structures and materials[42,59–62]. The main benefit of additive manufacturing technique is its ability to make multi-material parts during a single printing step, thus avoiding complicated assemblage processes.

Folding and assembly

Once the manufacturing is completed, the next step is to fold along the creases and assemble the folded components to achieve the final origami structure. Developable patterns, such as the Miura-ori, can be realized by folding a single flat sheet of material along the crease lines. By contrast, non-developable patterns, such as the Eggbox, can be obtained through the folding and assembling of several sub-parts or pieces[49]. In the case of paper-based origami, the union among different parts is usually achieved using flaps and either double-sided tape or paper glue. On the contrary, assembled plastic models are realized by glueing several modular base components. Conveniently, each unit cell or component should have several seats and/or extensions to allow an easy assembly.

Sample preparation and checks

The quality and integrity of the sample is fundamental for the success of the experiments. Some discrepancies between theoretical prediction and experimental results are commonly related to sample defects such as ageing, manufacturing and fatigue issues. For instance, if a crease is broken or damaged, an imperfection is introduced into the tessellation, deeply influencing the experimental results. For such reasons, before executing any mechanical test on origami tessellations (for example, uniaxial testing), a careful visual sample check should be done to verify the integrity of the pattern and its actual dimensions in the rest configuration should be verified with measuring devices (tape measure and caliper). In fact, the dimension of the sample in the rest configuration represents a common reference point for experiments,

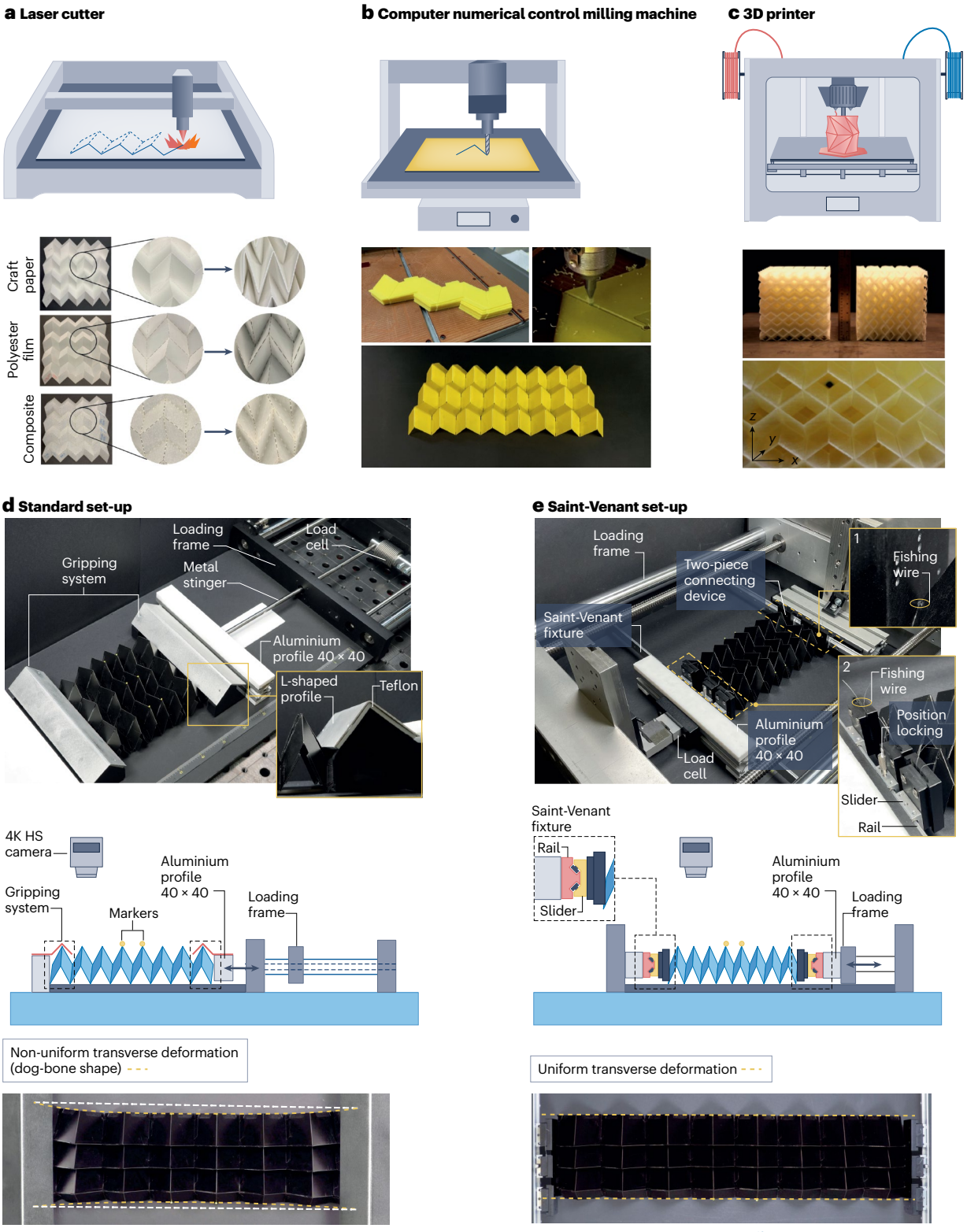

Fig. 2 | Origami experiments and manufacturing. a–**c**, Different manufacturing techniques used to create origami tessellation: paper and polymer-based origami models via laser cutting[47] (panel **a**), computer numerical control milled models realized using a milling machine[49] (panel **b**) and 3D printed models[5] (panel **c**). **d**,**e**, Set-ups adopted to perform uniaxial testing on origami tessellation: standard set-up (panel **d**) and Saint-Venant set-up[49] (panel **e**). The Saint-Venant set-up allows the sample to freely expand or contract in the transverse direction during folding and unfolding. This effectively prevents the sample from assuming a dog-bone shape and, instead, simulates the behaviour of a periodic system during uniaxial testing. Parts **d** and **e** adapted with permission from ref. 49, Elsevier.

theory and simulations[49]. Thus, the dimensions of the sample are an essential parameter when load versus displacement experimental data are compared with theoretical or numerical simulations (for example, in MERLIN[63]).

Experimental set-ups

Origami tessellations are reconfigurable structures that exhibit simultaneous deformations in both the longitudinal and transverse directions. Further, origami systems can be highly stiff in certain directions and flexible in other directions[37]. Hence, different types of experimental apparatus and set-ups may be required to investigate the behaviour of origami structures depending on the nature of deformations and loading. Recently, experimental set-ups to perform the uniaxial tests have been proposed to demonstrate the unique Poisson's ratio behaviour of origami metamaterials[49]. In this work, it has been shown that the gripping mechanism, connecting the ends of the sample to the loading frame, plays a key role in the quality of the results obtained from the testing machine. The standard way to connect the sample to the loading frame is by clamping its ends to the machine, as shown in Fig. 2d. The drawback of this approach is that the gripping system prevents the free deployment of the pattern in the transverse direction, leading to non-uniform transverse deformation. This is evident by observing the shape assumed by the sample during tension and compression testing. In a tension test, the sample deforms into a dog-bone shape; in compression, it deforms into a barrel shape. The proposed gripping mechanism[49] consists of a system of rail and sliders that allows proper attachment of the sample while permitting free transverse motion during the folding/unfolding process, as shown in Fig. 2e.

Such a system, called a Saint-Venant fixture, eliminates Saint-Venant end effects during uniaxial testing experiments. This advanced set-up permits a free deployment of the constrained sample, thus ensuring that the origami tessellation remains truly periodic even when deformed in a tension or compression test. To obtain high-resolution quantitative information from experiments, a loading frame machine is required for folding/unfolding of the origami tessellation. The loading frame should be equipped with a load cell and a displacement transducer for recording the applied load as a function of the sample length. The whole experimental apparatus should be arranged horizontally to reduce gravitational effects and avoid out-of-plane instabilities that could arise during the experiments. Moreover, a Teflon plate should be placed underneath the sample to reduce friction and stick–slip phenomena. For the monitoring of the longitudinal and transverse deformation of the sample, a high-resolution camera must be placed orthogonally to the testing platform to record the experiments. This allows recording of the motion of a selected array of points, identified by coloured markers, via a digital imaging correlation and tracking method. To facilitate the post-processing analysis via digital imaging correlation, the colour of the markers should be chosen to enhance the contrast with the tessellation.

Different origami patterns may require different experimental set-ups. For instance, the Kresling pattern couples axial displacement (contraction/expansion) with twist, leading to non-rigid origami behaviour. To experimentally investigate this behaviour, fixtures that decouple the deformation modes are needed[64]. Figure 3 illustrates the experimental set-ups for either compression or torsion tests on individual Kresling cells as well as generic Kresling arrays. The arrays can be composed of an odd or an even number of cells, without any constraint on the chiral arrangement of any cell or group of cells. Both set-ups comprise two fixtures that connect the top and bottom surfaces of the Kresling origami to the loading frame machine, as illustrated in Fig. 3a. Both fixtures are equipped with multiple miniaturized magnets, ensuring connections between the Kresling and the loading frame, as shown in Fig. 3a,d. In both set-ups, the bottom fixture is the same and effectively restrains both rotational and axial movements, preventing any undesired rigid motion of the Kresling samples during the tests. Figure 3c,f shows the snapshots recorded during the experiments. During the tests, axial force and twisting moment are recorded using a force/torque sensor. Additionally, the axial displacement can be measured with a displacement transducer. For further details, the reader is referred to ref. 64.

Data collection and post-processing

The main data acquired during origami uniaxial testing are the load applied at one end of the sample, the length evolution of the sample and the transversal and longitudinal deformation during the folding/unfolding process. A data acquisition system usually consists of a load cell and a displacement transducer to collect loads and displacements, respectively. The acquisition system could be part of the loading frame used to perform the test or external to the testing machine. In the former case, the data acquisition is more straightforward but not as versatile as in an external system, where there are no limits on the number and type of transducers. In the case of an external acquisition system, it is common to use a cDaq (by National Instruments) or Arduino systems interfaced with a PC through software written either in LabVIEW or MATLAB/Simulink. Analysis of the experimental data (load/displacement) can be performed in a spreadsheet (such as Office Excel, LibreOffice Calc, IWork Numbers) or in programming languages (such as Mathematica, MATLAB or Python). A tailored experimental method is needed for monitoring the transversal and longitudinal deformation of the pattern together with the execution of the test. For this purpose, a digital imaging correlation analysis and tracking method is essential for the frame by frame analysis of the recordings of the experiments and for estimating the motion of the markers previously located on the vertices of the pattern unit cell. Several strategies can be adopted to perform this analysis. The simplest way is manually analysing a limited number of frames extracted from the recorded movie through open-source software (for example, VLC, Quick Time combined with GIMP, or nanoCad). If a frame by frame analysis of the movie is required, this can be performed by ImageJ filament open-source software or through in-house software written in Mathematica, MATLAB or Python.

Actuation

The process of shape morphing in origami tessellations necessitates the utilization of external sources for actuation. The most employed methods for actuating origami structures include pneumatic actuation and magnetic actuation. However, the emergence of 4D printing has introduced the possibility of using stimuli-responsive materials that can respond, for instance, to light, heat or humidity (hygroscopic control).

Fluidic actuation. Fluidic actuation of origami involves using pressurized air or gas to control and manipulate origami structures[51]. In this context, as the origami samples need to be inflated they must be made impermeable to prevent air leakage. Typically, this is accomplished by coating origami structures with a thin layer of polydimethylsiloxane or by manufacturing them using plastic sheets with creases engraved onto them. To operate this method, the structure must be linked to an air supply system, such as a compressor or a simple air pump. This system allows for the regulation of both air pressure and flow rate. As this actuation approach is tethered, the structure being activated

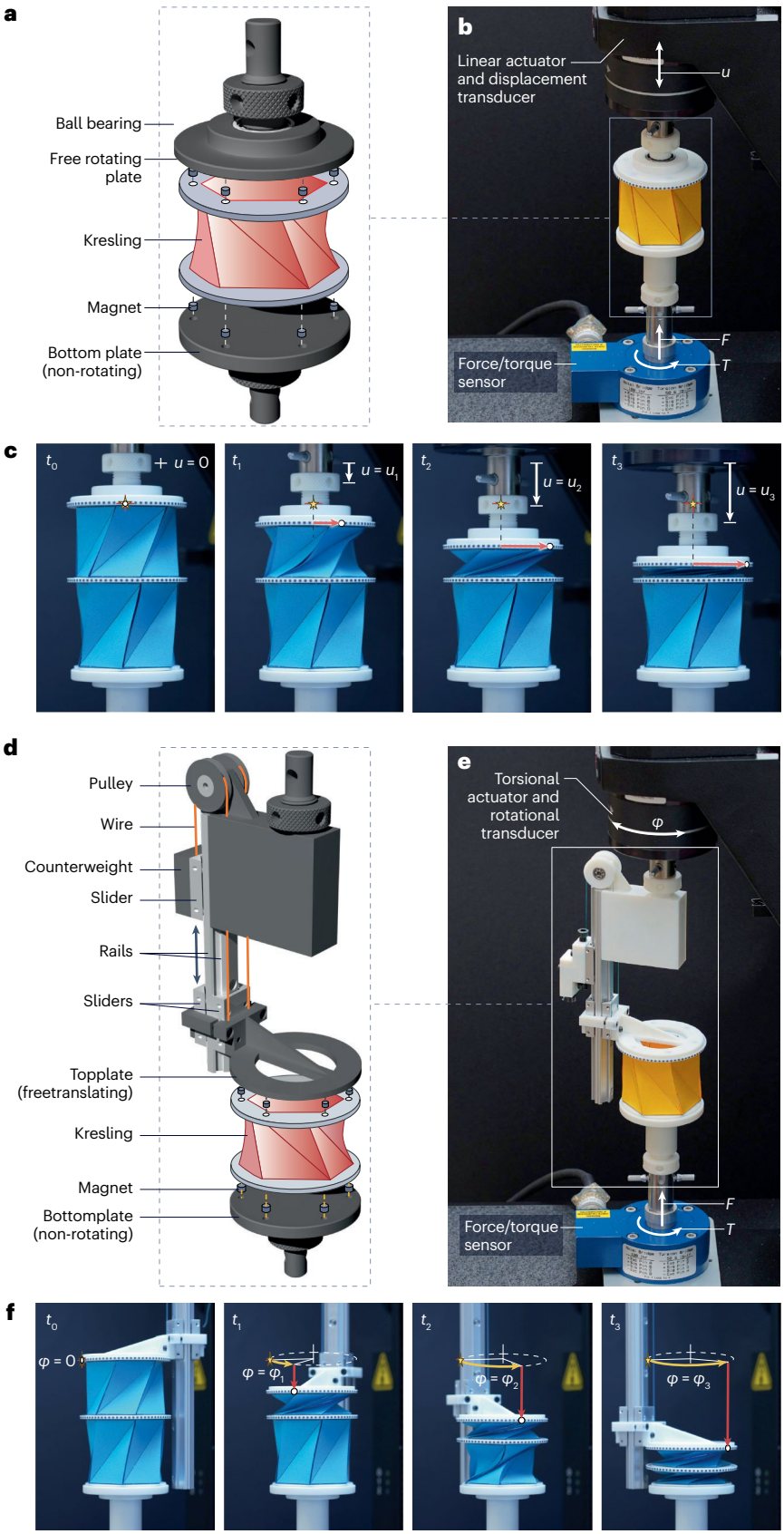

Fig. 3 | Set-up designed for conducting compression and torsion experiments on the Kresling origami. **a**–**f**, Free-rotating fixture (panel **a**) and free-translating fixture (panel **d**), set-ups in panels **a** and **d** mounted on the loading frame machine (panels **b** and **e**) and extracts from the record of the experiment at different times (panels **c** and **f**). The fixture in panel **c** enables free rotation that enables twisting of the Kresling cell (indicated by red arrows), whereas the fixture in panel **f** is attached to a linear slide system that enables unrestricted translation, allowing the Kresling array to undergo axial folding (indicated by red arrows). Adapted with permission from ref. 64, Elsevier.

needs to be equipped with an inlet for connecting the air source to the origami structure through flexible tubing.

Magnetic actuation. Magnetic actuation involves the utilization of magnetic fields to govern and manipulate origami structures that are crafted from materials that respond to magnetic forces[65,66]. This is accomplished by integrating magnetic components into the origami structures, which are magnetized beforehand. Usually, these magnetic components are created by blending a silicone rubber precursor with specific proportioning of magnetic microparticles. The magnetic characteristics of these components are determined using a magnetometer. Subsequently, actuation is typically achieved using, for example, a 3D Helmholtz coil system capable of generating a uniform magnetic field, the direction and intensity of which can be altered by adjusting the current flowing through the coils. The primary advantage of this method is that it enables untethered control with fast actuation.

Results

Typical properties exhibited by origami tessellations are characterized by tunability and programmability. Tunable properties arise by virtue of the various folded states of the system and can be changed through the application of an active stimulus (for example, force). The compliant folding of origami structures enables in situ control of the property they exhibit, making them excellent candidates for tunability. It has been demonstrated that several important mechanical properties, such as Poisson's ratio[30,31], elastic band gaps[44,67], thermal expansion coefficients[68] and anisotropic stiffness[37,69], can be tunable in origami metamaterials. As the folding of origami is generally a smooth continuous process, the variation in the properties that are being tuned is also gradual. Programmability, on the other hand, refers to obtaining a property of interest based on variations in the design (for example, geometry). This enables an abrupt change in the properties of the origami tessellation with respect to the change in the programmability parameter[70]. Programmability parameters are typically associated with the geometric features of the panels or local defects that can be induced in the origami tessellations. In this section, the theoretical geometric results pertaining to kinematics of origami patterns, modelling frameworks of non-rigid origami and some relevant properties (Poisson's ratio, wave dynamics and multistability) are addressed.

Geometry of representative origami patterns

The configuration of an origami structure is characterized by its crease pattern as well as the dihedral angle between panels that define the folded state. The edges of the panels correspond to the folding creases or boundaries of the structure, and the points of intersection of the creases are the vertices. The configurational analysis of origami can be carried out using concepts of spherical trigonometry to determine direct relations between the dihedral angles of the creases meeting at a vertex[71], and further determine the DOFs of the vertex. The DOFs of the entire origami structure, which may comprise several vertices, can be found using compatibility constraints imposed on the creases connecting adjacent vertices.

The Miura-ori pattern. The Miura-ori pattern was originally designed for use in space applications such as deployable solar arrays[72]. The pattern can also be found in certain plant leaves in nature[73]. The Miura-ori is a periodic 2D tessellation (or lattice) with each unit cell having four parallelogram-shaped panels as shown in Fig. 4. The Miura-ori pattern is composed of degree-four vertices where each vertex has either three mountain folds and one valley fold or vice versa. The angle α denotes the smaller panel angle (Fig. 4). When all the panels are rigid, the Miura-ori pattern possesses a single DOF. All the dihedral angles between adjacent panels depend on one single arbitrary folding angle, such as the crease angle ϕ as shown in Fig. 4. The crease angle (ϕ or ψ) uniquely describes any partially folded state of the structure. In the fully developed state, all the dihedral angles are equal to π. In the completely flat-folded state, the dihedral angles are either 0 or 2π and the structure is rigid. The relation between the two crease angles (ϕ and ψ) of the Miura-ori is given by:

$$\cos\left(\frac{\psi}{2}\right)\sin\left(\frac{\phi}{2}\right)=\cos\alpha \tag{7}$$

The eggbox pattern. The eggbox pattern takes its name from its appearance in the partially folded state. The eggbox is a 2D tessellation formed with two types of degree-four vertices that are non-developable. One of the vertices has four mountain (or valley) creases. The other vertex has two mountain creases and two valley creases. The pattern has parallelogram-shaped panels arranged in a fully symmetric way as shown in Fig. 4. When all the panels are rigid, the eggbox pattern deforms as a deployable single-DOF structure. The eggbox pattern exhibits smooth folding from one flat-folded state, where two dihedral angles are zero and the other two are π, to the other flat-folded state where the dihedral angles swap the values. Similar to the Miura-ori, the relation between the crease angles (ϕ and ψ) of the eggbox is given by:

$$\cos\left(\frac{\psi}{2}\right)\cos\left(\frac{\phi}{2}\right)=\cos\alpha \tag{8}$$

The waterbomb pattern. The most widely studied waterbomb origami[74] comprises degree-six vertices, as shown in Fig. 4. Depending on the tessellation, the degree-six waterbomb unit cell can fold in different curved configurations. Figure 4 shows the tessellation of a waterbomb unit cell with four mountain and two valley creases intersecting at a common vertex[75]. In general, the degree-six waterbomb unit cell has three DOFs. However, if the folding mode is restricted to be locally symmetrical (four mountain creases with the same dihedral angle), then the configuration of the structure at any partially folded state can be obtained from a single folding angle chosen as an independent variable. The relation between the folding angles ξ and γ is given by[76]:

$$\tan\left(\frac{\xi}{2}\right)=-\frac{1}{\cos\alpha}\tan\left(\frac{\gamma}{2}\right) \tag{9}$$

The Kresling tube. The triangulated cylinder/tube of the Kresling pattern undergoes non-rigid folding. The tessellation is formed by connecting unit cells along one direction as shown in Fig. 4. The crease pattern of a single unit cell is shown in Fig. 4 and is characterized independently by the parameters a, b, α and n, where n represents the number of edges (or cells) in each unit cell. The parameter c is also defined as shown in the figure. The unit cell can exhibit bistability depending on its geometric parameters and materials. The two stable states of the unit cell are denoted zero and one, and the corresponding folded configurations are characterized by the twist angles ψ_0 or ψ_1, respectively, and the unit cell heights h_0 or h_1, respectively. The two stable states are characterized by a geometric equivalence of the crease pattern parameters a, c and α. Therefore, enforcing these parameters

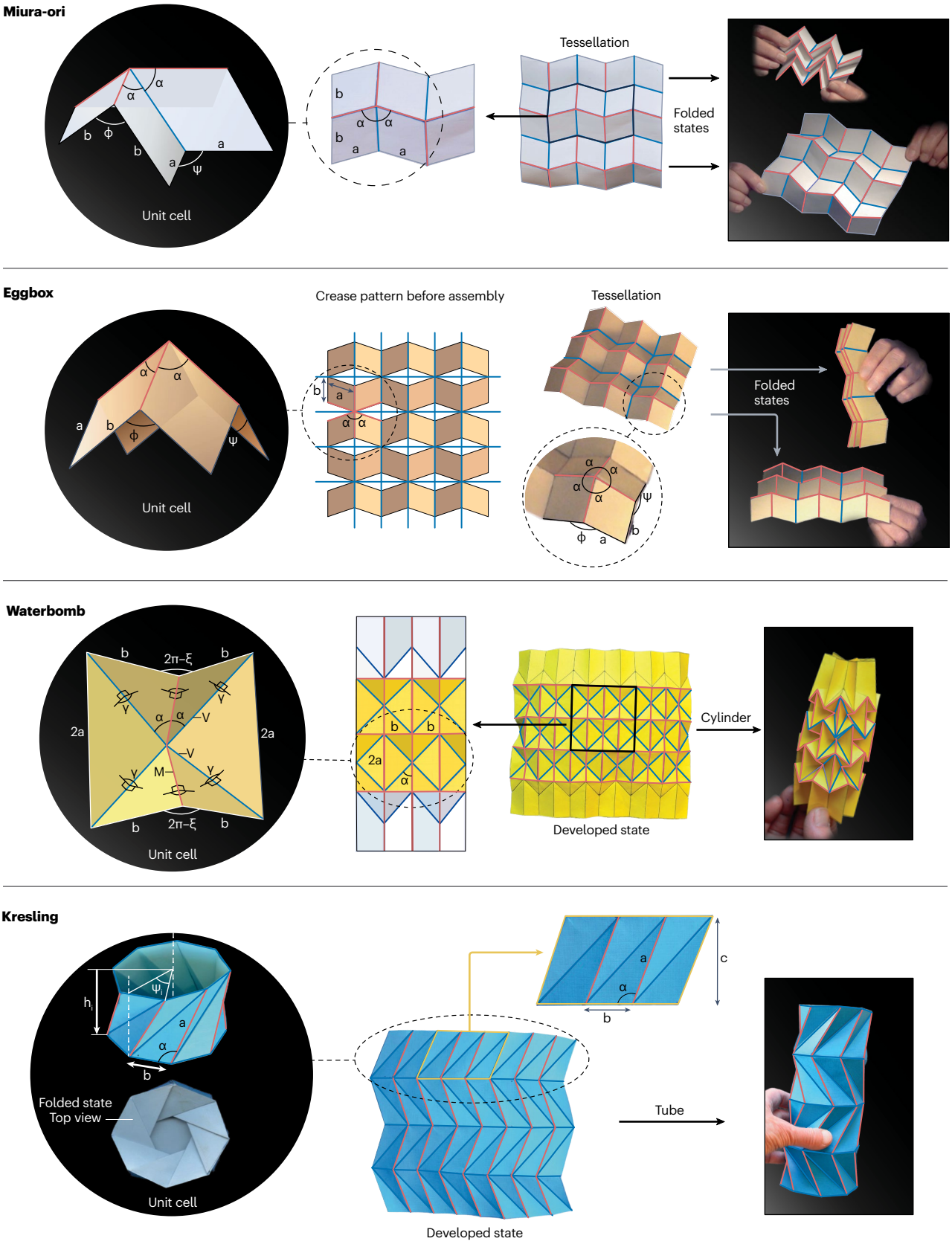
Miura-ori
Unit cell
Tessellation
Folded states
Eggbox
Crease pattern before assembly
Tessellation
Unit cell
Folded states
Waterbomb
Unit cell
Cylinder
Developed state
Kresling
Folded state
Top view
Unit cell
Tube
Developed state

Fig. 4 | Representation of the fusion of geometry, mathematics and art through origami tessellations. The unit cell, which forms the basis of the four tessellations considered, with geometrical parameters dictating their mechanics and configurations (left column). Miura-ori (from left to right): unit cell, unit module, tessellation in a deployed state and two images showcasing different folded states of a physical Miura-ori tessellation. Eggbox: non-developable nature of the pattern illustrated by its unit cell (left) requires that several strips cut from a flat sheet (middle-left) be assembled and glued together to obtain the desired tessellation (middle-right). Different folded states of a physical eggbox tessellation (right). Waterbomb (from left to right): unit cell, unit module, crease pattern and folded state. Kresling (from left to right): perspective and folded state top views of an eight-sided polygon unit cell, and one-piece crease pattern with reverse crease directions used to create the four-storey Kresling tube (right). a, b, side lengths; α, panel angle; ξ, γ, folding angles; φ, ψ, crease angles; c, height of the pattern; h, height of the Kresling unit cell; $i\,(h_i, \psi_i)$, 0 or 1 for the two stable states; M, mountain assignment; V, valley assignment.

to be the same in the two stable states, they can be calculated[71] as follows:

$$\alpha = \cos^{-1}\left(\frac{x_0\left[x_0 - \cot\left(\frac{\pi}{n}\right)\right]}{\sqrt{(x_0^2+1)\left[\left(\frac{h_0}{b}\right)^2(x_0^2+1) + x_0^2\csc^2\left(\frac{\pi}{n}\right)\right]}}\right) \tag{10}$$

$$a = b\sqrt{\left(\frac{h_0}{b}\right)^2 + \frac{x_0^2\csc^2\left(\frac{\pi}{n}\right)}{x_0^2+1}} \tag{11}$$

$$c = \frac{b\sqrt{\left(\frac{h_0}{b}\right)^2(x_0^2+1)^2 + x_0^3\cot\left(\frac{\pi}{n}\right)\left[x_0\cot\left(\frac{\pi}{n}\right)+2\right] + x_0^2}}{x_0^2+1} \tag{12}$$

$$x_{0,1} = 2\sin\left(\frac{\pi}{n}\right)\left[\frac{\sin\left(\frac{\pi}{n}\right)\sqrt{\cot^2\left(\frac{\pi}{n}\right)\csc^2\left(\frac{\pi}{n}\right) - [\tilde{h}]^2} - \cos\left(\frac{\pi}{n}\right)}{1 \mp \tilde{h} + [1 \pm \tilde{h}]\cos\left(\frac{2\pi}{n}\right)}\right] \tag{13}$$

with $\tilde{h} = (h_1/b)^2 - (h_0/b)^2$. The twisting angles for the two stable configurations are given by $\psi_0 = 2\tan^{-1}x_0$ and $\psi_1 = 2\tan^{-1}x_1$.

Structural analysis of origami

Some of the pioneering studies on origami structures focused on their rigid origami kinematics, which are of key interest for deployable structures and robotic applications. Some well-known software in this category includes the Rigid Origami Simulator that runs a projection-correction algorithm for solving linearized compatibility equations[22], the GPU-accelerated Origami Simulator[77] and the Rhino plug-in Crane[78].

However, in the past decade, interest in the use of origami for mechanical and civil engineering applications such as energy absorption, vibration control and load-bearing has gained prominence. Investigation of origami for such applications requires modelling the non-rigid behaviour of origami and carrying out structural analysis simulations. Besides shell-based finite element analysis, structural analysis of origami is typically carried out using an efficient reduced order model called the bar and hinge model[79], which captures the folding deformations, bending of panels and in-plane stretching of panels. In this model, the panels are replaced by bars that are placed along all the creases of the origami pattern as well as the panel diagonals. The stiffness associated with folding and panel bending is modelled through rotational springs or hinges between the triangulated truss-type panels. Some of the first bar and hinge models[79] were formulated to capture small deformations of origami tessellations during structural analysis. Later, improvements were made to bar and hinge models to capture various features such as isotropic panel stretching[37], complex panel-bending deformations and large non-linear deformations[63]. For example, Fig. 5a shows bending of an eggbox tessellation using MERLIN software that implements a non-linear mechanics formulation associated with the bar and hinge model[63]. Figure 5b shows representative simulation results by MERLIN, obtained from a uniaxial tension test of origami tessellations, that show good agreement with experimental data.

Poisson's ratio

Poisson's ratio is an important property that dictates the deformation of materials. The magnitude of Poisson's ratio of linear elastic isotropic materials is restricted within a small range from −1 to +0.5. Interestingly, origami metamaterials can exhibit Poisson effects that vary with the folded geometry of the structure[30] and are beyond the conventional range as they are typically not isotropic. For example, the Miura-ori pattern can exhibit in-plane Poisson's ratio values all the way from negative infinity to zero, achieving the extreme values when it is in a developed state or the flat-folded state. The negative Poisson effect in Miura-ori makes it an auxetic metamaterial. On the other hand, the eggbox pattern displays tunable in-plane Poisson's ratio values from zero to positive infinity as it folds from one flat-folded state to the other. The Poisson's ratio results for Miura-ori and eggbox origami metamaterials are shown in Fig. 5b, where good agreement between theory and experiments is obtained. Recently, novel origami patterns were discovered, namely Morph[31] (see Fig. 5b) and Trimorph[32], which can exhibit any real value of Poisson's ratio (negative infinity to positive infinity) depending on their folded configuration. Origami metamaterials exhibit a wide variation in the value of Poisson's ratio as they are being folded or deformed. However, recent research has shown that it is also possible to design origami patterns in such a way that the Poisson's ratio value is held nearly constant under large deformations[80]. All these results indicate the capability of origami metamaterials to be programmed or tuned to display desired Poisson effects.

Wave dynamics

Origami metamaterials have two major features that are useful for applications related to wave propagation and vibrations. First, the high contrasting levels of stiffness in the system in terms of crease folding, panel bending and panel stretching can lead to elastic band gaps, which denote ranges of frequencies where waves do not propagate. Second, the frequency range of the band gaps and other related characteristics can be easily tuned by compliant folding of origami. A technique called Bloch wave reduction can be employed to carry out wave propagation studies in periodic media such as origami tessellations[44]. Although typical calculations to study dynamics of tessellated structures could involve the consideration of several unit cells, the Bloch wave approach reduces the calculation effort to a single cell within the periodic system by virtue of its translational symmetry.

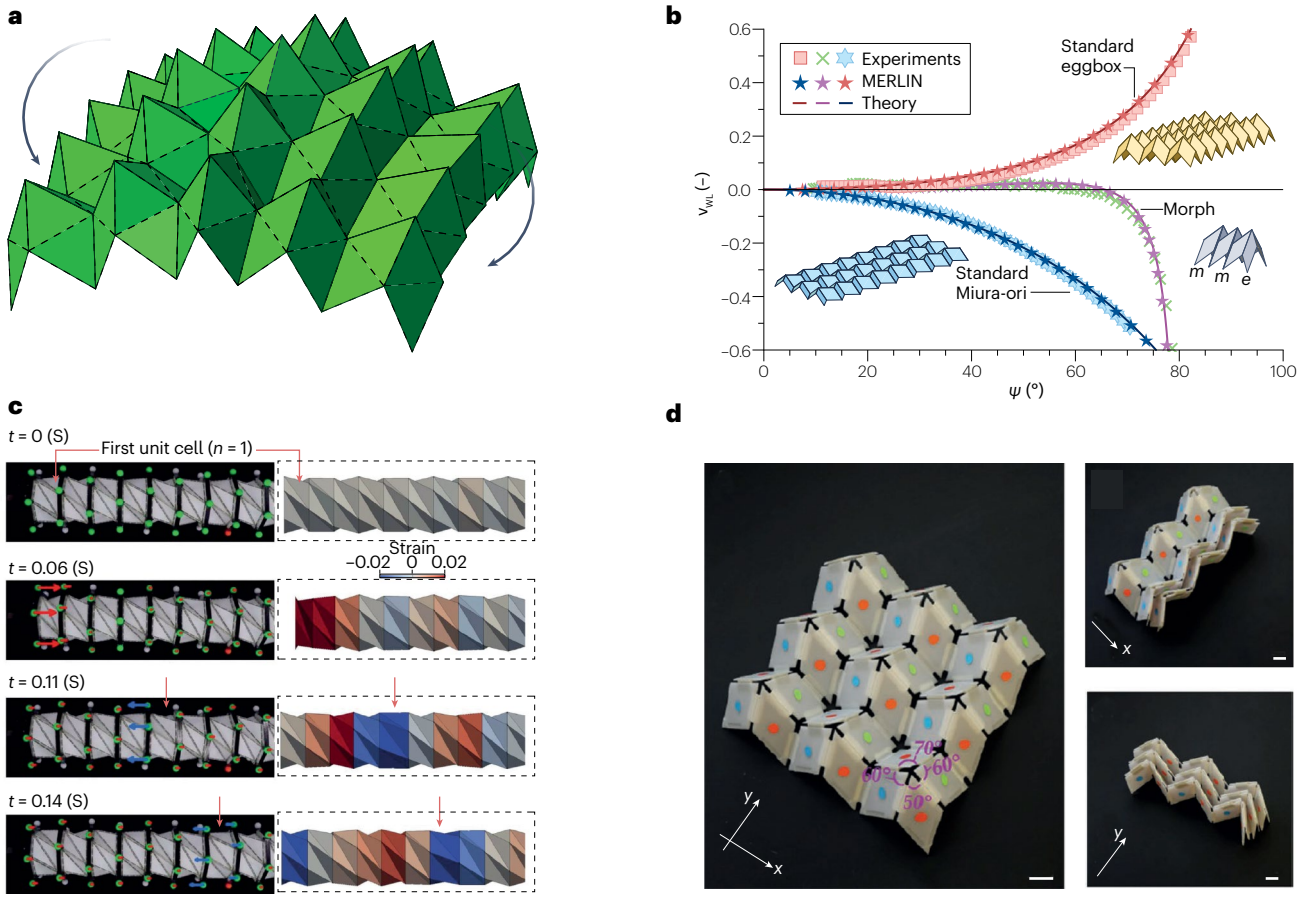

Fig. 5 | Mechanics of origami structures. a, Structural analysis of origami using MERLIN software. **b**, Poisson's ratio results of the Miura-ori, eggbox and morph origami metamaterials from theory, experiments (all experiments use 3 × 7 units) and MERLIN simulations. The Poisson's ratio variation for Miura-ori is negative and for eggbox is positive. The morph pattern is composed of seven layers, each having two units in the Miura-ori mode and one unit in the eggbox mode (see inset), and exhibits a Poisson's ratio switch from positive to negative. **c**, Wave propagation in Kresling tube origami. **d**, Different multistable states of Trimorph origami. Scale bar, 20 mm. ψ, crease angle; V_{WL}, Poisson's ratio. Part **b** adapted with permission from ref. 49, Elsevier. Part **c** reprinted with permission from ref. 45, AAAS. Part **d** reprinted with permission from ref. 32, Wiley.

Unlike several lattice structures, where the structural interactions are restricted to the nearest neighbouring nodes of a unit cell, origami metamaterials may exhibit non-local structural behaviour[44]. Hence, the application of Bloch boundary conditions should be careful enough to ensure that such (beyond nearest neighbour) nodal interactions are considered for accurate prediction of dynamic properties. Using such an approach, researchers have studied wave dynamics and band-gap structures in origami metamaterials. For example, modal characteristics of standard Miura-ori and eggbox patterns revealed the presence of elastic band gaps that are tunable by virtue of their folded configuration and programmable by virtue of their panel geometry[44]. That is, the frequency ranges of the band gaps obtained could be controlled (in theory) by subjecting the origami tessellation to folding, or by redesign of panel sizes or angles. In another study on wave dynamics, 1D origami-based lattice structures with triangulated cylinders were designed and experimentally found to exhibit rarefaction waves for applications in impact mitigation[45], as shown in Fig. 5c. There are two aspects that influence the tunable dynamic properties of origami lattice structures: the tunable geometry of the system by virtue of folding; and the mass and stiffness of panels and hinges. The former aspect is typically independent of the base material with which the origami structure is made. The latter aspect depends on the material used, and therefore influences the natural frequency ranges and, to some extent, the modal characteristics. Hence, the material should be chosen based on the target frequencies relevant to the engineering application. However, the tunability of the dynamic properties can be explored as a function of the choice of base material.

Multistability

Some origami structures experience multiple stable states such that each of them locks a particular configuration. These structures with multiple stable states can serve as the basic unit cell for architected materials, creating properties that differ from those of traditional materials. For example, the snap-through action (for example, the deformation process between different stable states) of the Kresling origami can be activated by non-contact forces, such as those generated by magnetic fields[46]. In addition, the multistable origami concept can be used to create a tessellation with switchable mechanical properties:

the Trimorph pattern, made by tessellation of tristable origami unit cells, can switch between different metastable phases to produce distinct stiffness, anisotropy and Poisson's ratio[32], as shown in Fig. 5d.

Conceptually, the multistability in origami structures usually comes from two types of incompatibility. The first is the incompatibility between the stress-free states of the folding hinges between the origami panels. This happens when the zero-energy, stress-free states of the folding hinges (or rest angles) of an origami structure are not compatible with its rigid folding kinematics, such that the folding hinges can never be all stress-free at the same time[81]. The second type is the incompatible panel geometries that forbid rigid folding, such as the square twist, Kresling pattern and many others[11,36,45,46,70,82]. Overcoming rigid foldability requires bending and stretching of the panels, which creates energy barriers between stable states where panels are usually flat and unstretched. Both types of incompatibility could be present in one pattern, at the same time, such as in the Trimorph pattern, in which the line defect is caused by the first source whereas the point defect is caused by the second source[32].

Applications

Owing to the inherent cross-disciplinary nature of its design principles, origami is a rich source of inspiration for creating cutting-edge materials and structures with a broad range of applications. A particular example of successful engineering application is foldcore sandwich panels[83]. A non-exhaustive list includes applications in engineering[15], physics[31], material science[30], microrobotics[84], waveguiding[85], impact mitigation[45], space structures (starshade origami), solar technologies[86] and artificial muscles[87]. Some distinguishing characteristics of origami are scalability and high deployability[84,88–90]. Scalability broadens the spectrum of applications across multiple length scales as the behaviour of origami structures is primarily governed by geometry in several cases. High deployability enables extremely reconfigurable shapes and tunable mechanical properties in static and dynamic regimes to be achieved. Thus, origami principles can inspire design of materials and structures with myriad applications[87,91–93]. Origami has generated ideas for futuristic infrastructure development, has inspired the creation of several artificial materials concepts, including metamaterials, has been used to create soft robots and medical devices and has enabled efficient transport of large structures in space applications. It is to be noted that the application areas discussed below are not mutually exclusive. Applications towards one topic (for example, mechanical metamaterials or soft robotics) can have relevance to applications related to another topic (for example, infrastructure or medical devices).

Sustainable and resilient infrastructure

Novel origami-based mechanisms have been implemented in architecture to create responsive building skins and adaptive diagrid façades capable of maximizing solar shading, acoustic performance, energy efficiency and structural performance[86,94]. The energy efficiency interventions on buildings, such as wall insulation, usually remain fixed over time regardless of the climatic conditions. On the contrary, the use of kinetic origami-based building skins can lead to maximizing energy efficiency at all hours of the day, optimizing the relation between internal comfort and exterior climate conditions. For example, some studies showed that kinetic origami-based facades optimize daylight by approximately 50% from March to September and about 30% from October to February, compared with the case of static façades, thus improving indoor visual and thermal comfort[95,96]. Another example is the futuristic shape-adaptive shading origami-based system installed on the facades of Al Bahar Towers, located in the financial centre of Abu Dhabi[97,98]. The motile façade installed on these towers reduces the internal temperature by 50% with a substantial decrease in energy consumption for air conditioning, diminishing CO_2 emissions by 1,750 tons per year[99]. Furthermore, origami-based systems are starting to be used to create kinetic solar arrays capable of tracking sun motion and, thus, maximizing solar energy intake[100,101].

Origami principles of reconfigurability and deployability can offer a valuable contribution to creating robust and resilient buildings, potentially minimizing material usage, thus leading to a dramatic reduction of embodied CO_2 emission[96,102,103]. In this context, there have been several efforts by researchers to obtain large-scale deployable structures inspired by origami behaviour. For example, pneumatic and multistable origami structures have been shown to allow the design of large-scale structures that can be deployed from a very compact configuration[33], as shown in Fig. 6a (top). Another example involves lightweight canopy structures that can be realized by coupling and stacking of origami tubes in different directions[37], as shown Fig. 6a (middle). This leads to deployable roofs with high out-of-plane stiffness. Other researchers used modified geometries to create novel accordion-type shelters with improved structural stability and stiffness[104], as shown in Fig. 6a (bottom).

Mechanical metamaterials

Metamaterials are artificial materials that can exhibit exotic properties superior to constituent materials[105]. Mechanical metamaterials are a subclass of metamaterials whose properties of interest are mechanical in nature, such as acoustic, thermal or elastic. Typically, metamaterials are obtained by repeating a unit cell whose geometry is designed once and cannot vary over time. Contrastingly, origami can transform its geometry continuously from a folded to an unfolded configuration, thus widening the design space. As metamaterial properties are strictly related to the unit cell geometry, origami permits achieving extremely tunable and reprogrammable mechanical properties[106–108]. Moreover, the relationship between stiffness of the panels and the creases provides opportunities to design the energy landscape of the resultant metamaterials[109–111]. This is useful to attain multistability, self-deployment or mechanical computing systems[112]. Origami design principles have also been successfully applied to conceive origami-based metamaterials exhibiting auxetic behaviour[30,113,114], tunable Poisson's ratio[36,38], self-locking[115,116], high strength-to-weight ratio[117,118] and tunable stiffness[39,111,119,120]. Some researchers have shown that, by properly designing kinematic paths, it is possible to achieve lockable and flat-foldable modes[38,121] (Fig. 6b). In addition to extreme static mechanical properties, origami-based metamaterials permit the achievement of tunable dynamic properties. For instance, the morphing of the origami tessellation leads to controlling electromagnetic or elastic waves[122,123], deflecting light[124], and opening and widening band gaps[44,85,125–127]. Origami metamaterials can also exhibit interesting coupling behaviours that are not typically observed in conventional materials, such as shear–normal coupling[32] and compression–twist coupling effects[128].

Soft robotics

In recent years, origami has been a source of inspiration for several applications in robotics. Soft robotics applications require gradual changes in stiffness and reconfigurability. Origami structures are well known to exhibit multistability, tunable stiffness and shape morphing, and hence can meet the design requirements for soft robotics. Exploiting origami-based design principles, robotic arms have been realized

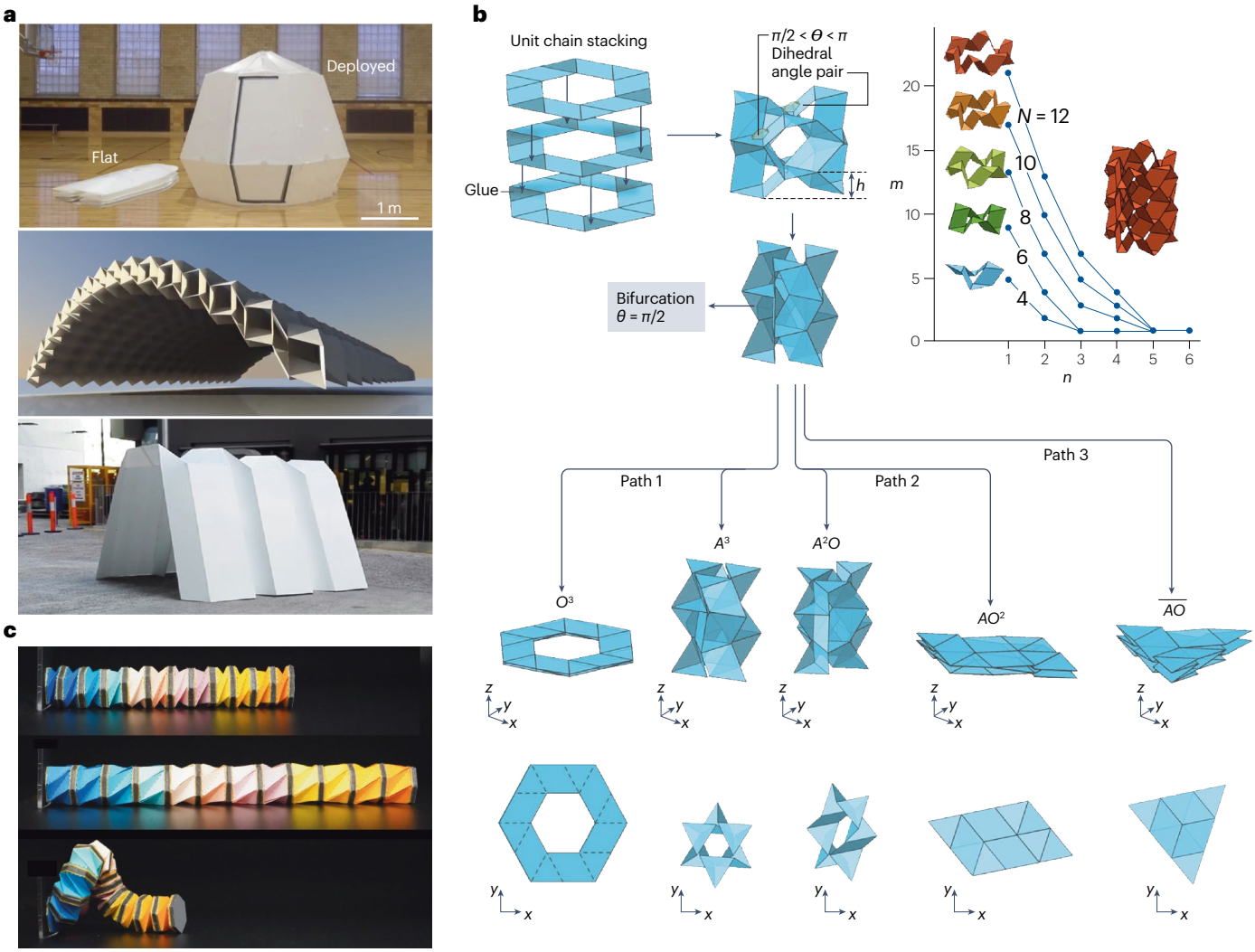

Fig. 6 | Origami applications. a, Examples of origami-based canopies and shelters. **b**, Multiple kinematic paths leading to lockable and flat-foldable modes in 3D origami-inspired metamaterials. **c**, Omnidirectional origami robot arm obtained by assembling several Kresling basic units, controlled via magnetic actuation. Part **a** (top) reprinted from ref. 33, Springer Nature Limited. Part **a** (middle) reprinted with permission from ref. 37, PNAS. Part **a** (bottom) reprinted with permission from ref. 104, ASME. Part **b** reprinted from ref. 38, Springer Nature Limited. Part **c** reprinted from ref. 129, CC BY 4.0.

through the uniaxial repetition of Kresling unit cells capable of multidirectional morphing, grasping objects and exploring hard-to-reach areas via magnetic actuation[46,65,129,130], as shown in Fig. 6c. Within this framework, origami morphing capabilities allow the realization of grippers[131], artificial hands that gently grasp fragile objects without breaking them[132–134]. Origami design principles can also inspire the creation of programmable artificial muscles with multidimensional actuation[87]. Origami robots capable of multimodal deformations[51,129] and navigation (for example, crawling, jumping and swimming) indicate the potential for advanced applications in this field.

Medical devices

The progress in rapid prototyping technology and the rising demand for increasingly miniaturized tools fostered the implementation of origami design in the biomedical industry for in vivo or ex vivo purposes. The scalability, high deployability and extreme packaging capabilities of origami make them particularly suitable for minimally invasive medical devices[135,136]. The auxetic nature of several origami patterns permits the conception of novel surgical tools that can access the human body through a small incision, travel in a very compact state to the intervention destination and deploy in their functional shape to execute the surgery. Origami designs have been explored for facilitating the execution of biopsy[137], MRI-guided radiofrequency ablation and catheter insertion[138] or inspection of hard-to-reach sites[139]. Origami-based deployable surgical reactors have been designed for potential use in face-lift operations[140] and adopted to create novel orthopaedic implants[141,142] and tissue scaffolds[143,144]. Origami-based self-folding microrobots have been realized to enable encapsulation, gastrointestinal microsurgeries[145] and drug delivery[146]. Origami-based structures have been conceived to assist retinal microsurgery[89,147] and as a support system for optimizing the insertion of flexible instruments in robot-assisted procedures[148]. Within this framework, origami-based microgrippers

have been designed for the capture and retrieval of objects and biopsies[149,150], minimizing invasiveness and potential human errors.

Space technology

Space structures, such as solar arrays or satellites, are large-scale structures that need to be compactly transported and deployed in target orbits. Efficient transport of such structures requires them to be lightweight and able to be folded into a small volume. Origami patterns can be implemented in the design of extremely lightweight, densely packed membranes and devices to be deployed once placed at target locations in space. Deployable membranes can serve as solar sails, propelled by solar wind, for exploration missions; as solar power arrays for satellites, for solar energy collection, conversion and transmission; as reflect array antennas; as space telescopes; and as protective shields[151,152]. The Miura-ori pattern was a key invention that enabled compaction and deployment of space structures[72,153–155]. Design of origami-based solar sails has evolved over years, for example, with a different deployment technique that uses radial segments, wrapped in spirals around a central hub, that unfold tangentially[156]. The pattern resembles a moonflower just after opening, and is nicknamed 'origami flasher'[101,157,158] (starshade origami). Another variant, a four-quadrant square solar sail is extended in the diagonals by telescopic booms. The recent Kresling pattern[1,2,159,160] allows cylinders to be actively folded and unfolded, similar to bellows, and is applied to the Sunshield project of the IXO-Space Telescope[161], the Mars Rover drill protection and for origami antennas of space–ground communication[81].

Reproducibility and data deposition

Reproduction of samples

Physical samples of origami are made with various methods. In general, the kinematics of origami structures is primarily driven by its geometry and is less sensitive to the materials being used, which is one of the many virtues of origami designs. However, deviations in the geometric structure, such as misalignment in the crease pattern, could lead to discrepancy from the expected behaviour. In a previous study, experiments and numerical simulations showed that geometric imperfections could hinder the foldability of origami structures and increase its compressive stiffness[47]. This effect is less apparent when the origami

Glossary

Bird's feet condition
A single-vertex crease pattern can be rigidly folded if, and only if, it contains a bird's foot, where a set of three creases of the same mountain/valley (*M*/*V*) assignment are separated sequentially by angles strictly between 0° and 180°, plus one additional crease of the opposite assignment.

Bloch wave reduction
A discrete Fourier transformation-based technique that enables efficient analysis of infinitely periodic lattice systems.

Colouring
The crease pattern of a flat-foldable origami structure (for example, crane) can be coloured such that no two neighbouring regions are assigned the same colour while using as few colours as possible.

Crease pattern
The pattern of creases left on the surface after an origami structure has been unfolded.

Creases
Marks left on the material surface after a fold has been unfolded.

Degree-four vertices
Vertices delimited by four creases or four panels. For example, parallelogram-based origami is composed of degree-four vertices.

Developable
Origami that can be unfolded into a flat sheet without overlapping or deformation of the panels.

Dihedral angle
The angle between adjacent panels, which describes the current configuration.

Elastic band gaps
The frequency range within which elastic wave propagation is prevented through the medium.

Extensions
Appendages on the panels that can be placed and glued onto the matching seats.

Flat-foldable
Origami that can be folded into a flattened state of zero volume.

Foldcore
A sandwich structure consisting of thin stiff facesheets and thick, low-density core made of an architected material (for example, origami).

Folding angles
The angles that are required for one panel of an adjacent pair to rotate until it meets the other panel in a consistent direction, which could be either the dihedral angle or its supplementary angle.

Kirigami
The Japanese art of cutting and folding thin sheets of materials (for example, paper) from flat into three-dimensional objects.

Linkages
Mechanisms built from stiff bars connected by freely rotating joints (rigid links).

Origami
The art of folding paper (or other surfaces) into three-dimensional shapes, usually from uncut squares or other continuous shapes.

Panels
The basic elements of an origami structure that occupy the area bounded by creases or borders of the surface.

Poisson's ratio
The negative of the ratio of transverse strain to longitudinal strain in a material subject to uniaxial loading.

Right-hand thumb rule
A commonly used rule to determine direction of rotational quantities and associated vectors. Here, it is used to determine the direction or sign of the turning angles corresponding to an axis of rotation placed along the crease.

Rigid origami
Origami that can be folded while keeping all regions of the surface (for example, paper) flat and all crease lines straight.

Saint-Venant end effects
A small region near the point of load with non-uniform distribution of stress, where the effect of the exact form of the loading cannot be ignored.

Seats
Grooves made by material removal for precise placement of joints.

Tessellations
Coverings on a surface, using one or more patterns (tiles) with no overlaps and no gaps.

is made with compliant (or soft) materials but becomes severe for stiff materials. For Miura-ori, the square residual of the Kawasaki–Justin condition (for example, Kawasaki excess) correlates approximately linearly with the increase in stiffness of imperfect Miura-ori structures[47]. Small geometric imperfections stiffen the originally programmed mode but generally do not alter the mode shape.

Data deposition

Origami structures are usually shared in data formats that store meshes, which must include at least two pieces of information: the coordinates of the vertices (or nodes); and the groups of vertices that belong to each face (or panel). A typical example of such a format is the OBJ format, which is supported by the Rigid Origami Simulator[77], the Origamizer[162] and MERLIN[63]. Although the STL format is the most common for 3D printing and animation editing, it is not suitable for origami because all faces in STL must be triangular, whereas polygonal faces are common in origami designs. Recently, researchers formulated the flexible origami list data structure (FOLD) format that is dedicated to origami design[163]. Compared with the standard industrial formats, the FOLD format not only stores the static information of an origami design but also allows frames to be collected that depict the folding process of an origami structure. For flat-folded origami, the FOLD format includes the topological stacking order of faces that overlap geometrically to distinguish different folded states. The FOLD format is gradually becoming popular among the origami community. Origami Simulator[21] and MERLIN[63] support the FOLD format. Note that all formats mentioned above apply to both partially folded origami and its flat crease pattern.

Limitations and optimizations

Most current developments in origami engineering are based on an adaptation of existing origami patterns or are those that gained attention by serendipitous discovery. Principles-based systematic design of new origami patterns that can exhibit exotic engineering properties is a challenging problem. Although there have been developments in the recent years towards inverse design of origami for engineering applications, they are still in the rudimentary stages. The theoretical or numerical design of origami patterns for target requirements is an active area of research[164–166] and more developments are needed in this direction, to make origami engineering versatile across applications. The challenges arise from two contexts — one related to the choice of design variable space and the other related to the choice of engineering properties that are explored. Further, in most cases, the designs must satisfy requirements related to developability, flat foldability or rigid folding, which constraints the solution space. In terms of applications, the design of crease hinges, especially in the context of thick origami, is not systematically investigated and hinders large-scale and reliable use of origami structures made from thick sheets of material or thick-panel prisms.

Behaviour of origami patterns is particularly influenced by the presence of imperfections in their geometry. Most studies on origami patterns demonstrate the results through prototypes made from regular symmetric structures with no imperfections. However, the presence of geometric imperfections in the patterns can lead to unexpected behaviour. Hence, extensive studies by incorporating imperfections owing to manufacturing defects should be performed while investigating the suitability of origami for applications.

Limitations of efficient manufacturability of origami structures also exist, especially in the context of non-developable patterns. Most current methods involve manual assembling of individual modules to form the final tessellated structure. Further, in the context of developable patterns, the tessellated structures need manual folding through creases marked on the entire sheet. Advanced manufacturing techniques such as 3D printing can be investigated to seek potential alternatives to these limitations.

Exploring micro-scale sample experimentation remains a relatively unexplored territory demanding further investigation. From a mathematical point of view, origami structures exhibit scale-independent properties. However, from an engineering perspective, larger-scale experiments behave differently from micro-scale origami, as the process of miniaturizing origami introduces significant complexities, owing to the changing underlying physics governing the mechanical response at different scales. These complexities encompass various factors, including the substantial impact of Van der Waals forces on the mechanical response of micro-scale origami, the intricate challenges associated with manufacturing owing to limited materials and manufacturing technologies capable of achieving nanometre precision, as well as the development of miniature testing platforms.

Origami structures can be highly kinematic in nature with multiple DOFs. Thorough analysis of the structure's mobility should be carried out before adapting origami for applications. If unwanted modes of mobility are found to exist, appropriate constraints should be applied on the structure to lock or guide it into desired configurations.

Outlook

Although origami science is a more mature field, origami engineering has the potential to revolutionize the fields of engineering and design by enabling the creation of complex, lightweight and adaptable structures across scales, which can be manipulated and deployed in various applications. Beyond modelling and manufacturing of origami, automated folding and actuation can lead to major advances especially with multi-physics considerations (for example, magnetic actuation[46,167]). Thus, origami engineering has potential for continued advances in several fields ranging from robotics to space structures, architecture and medical technology. The latter field holds great potential, especially as medical doctors and engineers collaborate in a true interdisciplinary fashion including actual experiments in animals with potential for further findings in humans. Modelling of an origami structure is problem-specific, and therefore a single framework may not be readily applicable. Therefore, researchers have adopted context-specific modelling approaches for origami. As origami ideas permeate different fields, several origami modelling frameworks and packages are expected to be developed in the future. Alongside, one could expect various design approaches to also be developed. The material used to make the origami may play a key role and challenge the development of manufacturing processes for origami-based structures. Although many recent studies on origami use paper-based models to demonstrate ideas, real applications — depending on the length scale of interest — could use various materials ranging from polymeric materials at the micron scale[58] to construction materials such as steel or concrete[168] that could help reshape our infrastructure towards more sustainable solutions. Other fascinating materials to be explored are biological materials and living tissues, which could revolutionize the medical field[169].

Published online: 26 June 2024

References

1. Kresling, B. Origami-structures in nature: lessons in designing “smart” materials. *MRS Online Proceedings Library* **1420**, 42–54 (2012).
2. Kresling, B. Folded tubes as compared to kikko (‘tortoise-shell’) bamboo. *Origami* **3**, 197–207 (2002).
3. Foster, C. G. Some observations on the Yoshimura buckle pattern for thin-walled cylinders. *J. Appl. Mech.* **46**, 377–380 (1979).
4. Liu, K., Tachi, T. & Paulino, G. H. Invariant and smooth limit of discrete geometry folded from bistable origami leading to multistable metasurfaces. *Nat. Commun.* **10**, 4238 (2019).
5. Cheung, K. C., Tachi, T., Calisch, S. & Miura, K. Origami interleaved tube cellular materials. *Smart Mater. Struct.* **23**, 094012 (2014).
6. Hull, T. *Project Origami: Activities for Exploring Mathematics* (CRC, 2012).
7. O’Rourke, J. *How to Fold It: The Mathematics of Linkages, Origami, and Polyhedra* (Cambridge Univ. Press, 2011).
8. Demaine, E. D. & Joseph, O. R. *Geometric Folding Algorithms: Linkages, Origami, Polyhedra* (Cambridge Univ. Press, 2007).
9. Ma, J., Zang, S., Feng, H., Chen, Y. & You, Z. Theoretical characterization of a non-rigid-foldable square-twist origami for property programmability. *Int. J. Mech. Sci.* **189**, 105981 (2021).
10. Wang, L.-C. et al. Active reconfigurable tristable square-twist origami. *Adv. Funct. Mater.* **30**, 1909087 (2020).
11. Li, Y. & Pellegrino, S. A theory for the design of multi-stable morphing structures. *J. Mech. Phys. Solids* **136**, 103772 (2020).
12. Belcastro, S.-M. & Hull, T. C. Modelling the folding of paper into three dimensions using affine transformations. *Linear Algebra Its Appl.* **348**, 273–282 (2002).
13. Hull, T. C. *Origametry: Mathematical Methods in Paper Folding* (Cambridge Univ. Press, 2020).
14. Tachi, T. Generalization of rigid-foldable quadrilateral-mesh origami. *J. Int. Assoc. Shell Spat. Struct.* **50**, 173–179 (2009).
15. Peraza Hernandez, E. A., Hartl, D. J. & Lagoudas, D. C. *Active Origami: Modeling, Design, and Applications* (Springer, 2018).
16. J. Denavit, R. S. H. A kinematic notation for lower-pair mechanisms based on matrices. *J. Appl. Mech.* **22**, 215–221 (1955).
17. Chen, Y., Peng, R. & You, Z. Origami of thick panels. *Science* **349**, 396–400 (2015).
18. Chen, Y. & You, Z. *Motion Structures: Deployable Structural Assemblies of Mechanisms* (CRC, 2011).
19. Abel, Z. et al. Rigid origami vertices: conditions and forcing sets. *J. Comput. Geom.* **7**, 171–184 (2016).
20. He, Z. & Guest, S. D. On rigid origami I: piecewise-planar paper with straight-line creases. *Proc. R. Soc. Math. Phys. Eng. Sci.* **475**, 20190215 (2019).
21. He, Z. & Guest, S. D. On rigid origami II: quadrilateral creased papers. *Proc. R. Soc. Math. Phys. Eng. Sci.* **476**, 20200020 (2020).
22. Tachi, T. in *Origami 4* 1st edn, Ch. 16 (ed. Lang, R. J.) 175–187 (A K Peters/CRC Press, 2009).
23. Lang, R. J., Tolman, K. A., Crampton, E. B., Magleby, S. P. & Howell, L. L. A review of thickness-accommodation techniques in origami-inspired engineering. *Appl. Mech. Rev.* **70**, 010805 (2018).
24. Tachi, T. Rigid-foldable thick origami. *Origami* **5**, 253–264 (2011).
25. Edmondson, B. J., Lang, R. J., Magleby, S. P. & Howell, L. L. An offset panel technique for thick rigidily foldable origami. in *International Design Engineering Technical Conferences and Computers and Information in Engineering Conference* Vol. 46377 V05BT08A054 (American Society of Mechanical Engineers, 2015).
26. Gu, Y., Wei, G. & Chen, Y. Thick-panel origami cube. *Mech. Mach. Theory* **164**, 104411 (2021).
27. Ku, J. S. & Demaine, E. D. Folding flat crease patterns with thick materials. *J. Mech. Robot.* **8**, 031003 (2016).
28. Yang, J., Zhang, X., Chen, Y. & You, Z. Folding arrays of uniform-thickness panels to compact bundles with a single degree of freedom. *Proc. R. Soc. Math. Phys. Eng. Sci.* **478**, 20220043 (2022).
29. Lang, R. J., Nelson, T., Magleby, S. & Howell, L. Thick rigidly foldable origami mechanisms based on synchronized offset rolling contact elements. *J. Mech. Robot.* **9**, 021013 (2017).
30. Schenk, M. & Guest, S. D. Geometry of Miura-folded metamaterials. *Proc. Natl Acad. Sci. USA* **110**, 3276–3281 (2013).
31. Pratapa, P. P., Liu, K. & Paulino, G. H. Geometric mechanics of origami patterns exhibiting Poisson’s ratio switch by breaking mountain and valley assignment. *Phys. Rev. Lett.* **122**, 155501 (2019).
32. Liu, K., Pratapa, P. P., Misseroni, D., Tachi, T. & Paulino, G. H. Triclinic metamaterials by tristable origami with reprogrammable frustration. *Adv. Mater.* **34**, 2107998 (2022).
33. Melancon, D., Gorissen, B., García-Mora, C. J., Hoberman, C. & Bertoldi, K. Multistable inflatable origami structures at the metre scale. *Nature* **592**, 545–550 (2021).
34. Kaufmann, J., Bhovad, P. & Li, S. Harnessing the multistability of Kresling origami for reconfigurable articulation in soft robotic arms. *Soft Robot.* **9**, 212–223 (2022).
35. Lu, L., Dang, X., Feng, F., Lv, P. & Duan, H. Conical Kresling origami and its applications to curvature and energy programming. *Proc. R. Soc. A* **478**, 20210712 (2022).
36. Silverberg, J. L. et al. Origami structures with a critical transition to bistability arising from hidden degrees of freedom. *Nat. Mater.* **14**, 389–393 (2015).
37. Filipov, E. T., Tachi, T. & Paulino, G. H. Origami tubes assembled into stiff, yet reconfigurable structures and metamaterials. *Proc. Natl Acad. Sci. USA* **112**, 12321–12326 (2015).
38. Jamalimehr, A., Mirzajanzadeh, M., Akbarzadeh, A. & Pasini, D. Rigidly flat-foldable class of lockable origami-inspired metamaterials with topological stiff states. *Nat. Commun.* **13**, 1816 (2022).
39. Zhai, Z., Wang, Y. & Jiang, H. Origami-inspired, on-demand deployable and collapsible mechanical metamaterials with tunable stiffness. *Proc. Natl Acad. Sci. USA* **115**, 2032–2037 (2018).
40. Yasuda, H., Tachi, T., Lee, M. & Yang, J. Origami-based tunable truss structures for non-volatile mechanical memory operation. *Nat. Commun.* **8**, 962 (2017).
41. Kim, W. et al. Bioinspired dual-morphing stretchable origami. *Sci. Robot.* **4**, eaay3493 (2019).
42. Kotikian, A. et al. Untethered soft robotic matter with passive control of shape morphing and propulsion. *Sci. Robot.* **4**, eaax7044 (2019).
43. Mintchev, S., Shintake, J. & Floreano, D. Bioinspired dual-stiffness origami. *Sci. Robot.* **3**, eaau0275 (2018).
44. Pratapa, P. P., Suryanarayana, P. & Paulino, G. H. Bloch wave framework for structures with nonlocal interactions: application to the design of origami acoustic metamaterials. *J. Mech. Phys. Solids* **118**, 115–132 (2018).
45. Yasuda, H. et al. Origami-based impact mitigation via rarefaction solitary wave creation. *Sci. Adv.* **5**, eaau2835 (2019).
46. Novelino, L. S., Ze, Q., Wu, S., Paulino, G. H. & Zhao, R. Untethered control of functional origami microrobots with distributed actuation. *Proc. Natl Acad. Sci. USA* **117**, 24096–24101 (2020).
47. Liu, K., Novelino, L. S., Gardoni, P. & Paulino, G. H. Big influence of small random imperfections in origami-based metamaterials. *Proc. R. Soc. A* **476**, 20200236 (2020).
48. Xia, Y., Kidambi, N., Filipov, E. & Wang, K.-W. Deployment dynamics of Miura origami sheets. *J. Comput. Nonlinear Dyn.* **17**, 071005 (2022).
49. Misseroni, D., Pratapa, P. P., Liu, K. & Paulino, G. H. Experimental realization of tunable Poisson’s ratio in deployable origami metamaterials. *Extreme Mech. Lett.* **53**, 101685 (2022).
50. Mora, S., Pugno, N. M. & Misseroni, D. 3D printed architected lattice structures by material jetting. *Mater. Today* **107**, 132 (2022).
51. Melancon, D., Forte, A. E., Kamp, L. M., Gorissen, B. & Bertoldi, K. Inflatable origami: multimodal deformation via multistability. *Adv. Funct. Mater.* **32**, 2201891 (2022).
52. Mehrpouya, M., Azizi, A., Janbaz, S. & Gisario, A. Investigation on the functionality of thermoresponsive origami structures. *Adv. Eng. Mater.* **22**, 2000296 (2020).
53. Dalaq, A. S. & Daqaq, M. F. Experimentally-validated computational modeling and characterization of the quasi-static behavior of functional 3D-printed origami-inspired springs. *Mater. Des.* **216**, 110541 (2022).
54. Huang, C., Tan, T., Hu, X., Yang, F. & Yan, Z. Bio-inspired programmable multi-stable origami. *Appl. Phys. Lett.* **121**, 051902 (2022).
55. Qi, J., Li, C., Tie, Y., Zheng, Y. & Duan, Y. Energy absorption characteristics of origami-inspired honeycomb sandwich structures under low-velocity impact loading. *Mater. Des.* **207**, 109837 (2021).
56. Zhao, Z. et al. 3D printing of complex origami assemblages for reconfigurable structures. *Soft Matter* **14**, 8051–8059 (2018).
57. Zhao, Z. et al. Origami by frontal photopolymerization. *Sci. Adv.* **3**, e1602326 (2017).
58. Lin, Z. et al. Folding at the microscale: enabling multifunctional 3D origami-architected metamaterials. *Small* **16**, 2002229 (2020).
59. Fang, Z. et al. Modular 4D printing via interfacial welding of digital light-controllable dynamic covalent polymer networks. *Matter* **2**, 1187–1197 (2020).
60. Ge, Q., Dunn, C. K., Qi, H. J. & Dunn, M. L. Active origami by 4D printing. *Smart Mater. Struct.* **23**, 094007 (2014).
61. Xia, X., Spadaccini, C. M. & Greer, J. R. Responsive materials architected in space and time. *Nat. Rev. Mater.* **7**, 683–701 (2022).
62. Chen, T., Bilal, O. R., Lang, R., Daraio, C. & Shea, K. Autonomous deployment of a solar panel using elastic origami and distributed shape-memory-polymer actuators. *Phys. Rev. Appl.* **11**, 064069 (2019).
63. Liu, K. & Paulino, G. H. Nonlinear mechanics of non-rigid origami: an efficient computational approach. *Proc. R. Soc. Math. Phys. Eng. Sci.* **473**, 20170348 (2017).
64. Zang, S., Misseroni, D., Zhao, T. & Paulino, G.H. Kresling origami mechanics explained: experiments and theory. *J. Mech. Phys. Solids* **188**, 105630 (2024).
65. Sitti, M. *Mobile Microrobotics* (MIT Press, 2017).
66. Cui, J. et al. Nanomagnetic encoding of shape-morphing micromachines. *Nature* **575**, 164–168 (2019).
67. Thota, M. & Wang, K. W. Reconfigurable origami sonic barriers with tunable bandgaps for traffic noise mitigation. *J. Appl. Phys.* **122**, 154901 (2017).
68. Boatti, E., Vasios, N. & Bertoldi, K. Origami metamaterials for tunable thermal expansion. *Adv. Mater.* **29**, 1700360 (2017).
69. Mukhopadhyay, T. et al. Programmable stiffness and shape modulation in origami materials: emergence of a distant actuation feature. *Appl. Mater. Today* **19**, 100537 (2020).
70. Silverberg, J. L. et al. Using origami design principles to fold reprogrammable mechanical metamaterials. *Science* **345**, 647–650 (2014).
71. Lang, R. J. *Twists, Tilings, and Tessellations: Mathematical Methods for Geometric Origami* (CRC, 2017).
72. Miura, K. & Lang, R. J. The science of Miura-ori: a review. *Origami* **4**, 87–99 (2009).
73. Kobayashi, H., Kresling, B. & Vincent, J. F. V. The geometry of unfolding tree leaves. *Proc. R. Soc. Lond. B Biol. Sci.* **265**, 147–154 (1998).
74. Chen, Y., Feng, H., Ma, J., Peng, R. & You, Z. Symmetric waterbomb origami. *Proc. R. Soc. Math. Phys. Eng. Sci.* **472**, 20150846 (2016).

75. Randlett, S. *The Art of Origami: Paper Folding, Traditional and Modern* (EP Dutton, 1961).
76. Pratapa, P. P. & Bellamkonda, A. Thick panel origami for load-bearing deployable structures. *Mech. Res. Commun.* **124**, 103937 (2022).
77. Tachi, T. Design of infinitesimally and finitely flexible origami based on reciprocal figures. *J. Geom. Graph.* **16**, 223–234 (2012).
78. Suto, K., Noma, Y., Tanimichi, K., Narumi, K. & Tachi, T. Crane: an integrated computational design platform for functional, foldable, and fabricable origami products. *ACM Trans. Comput. Hum. Interact.* **30**, 1–29 (2023).
79. Schenk, M. & Guest, S. D. Origami folding: a structural engineering approach. *Origami* **5**, 291–304 (2011).
80. Vasudevan, S. P. & Pratapa, P. P. Origami metamaterials with near-constant Poisson functions over finite strains. *J. Eng. Mech.* **147**, 04021093 (2021).
81. Moshtaghzadeh, M., Izadpanahi, E. & Mardanpour, P. Prediction of fatigue life of a flexible foldable origami antenna with Kresling pattern. *Eng. Struct.* **251**, 113399 (2022).
82. Waitukaitis, S., Menaut, R., Chen, B. G. & van Hecke, M. Origami multistability: from single vertices to metasheets. *Phys. Rev. Lett.* **114**, 055503 (2015).
83. Sturm, R., Schatrow, P. & Klett, Y. Multiscale modeling methods for analysis of failure modes in foldcore sandwich panels. *Appl. Compos. Mater.* **22**, 857–868 (2015).
84. Tang, J. & Wei, F. Miniaturized origami robots: actuation approaches and potential applications. *Macromol. Mater. Eng.* **307**, 2100671 (2022).
85. Thota, M. & Wang, K. W. Tunable waveguiding in origami phononic structures. *J. Sound. Vib.* **430**, 93–100 (2018).
86. Tang, R. et al. Origami-enabled deformable silicon solar cells. *Appl. Phys. Lett.* **104**, 083501 (2014).
87. Li, S., Vogt, D. M., Rus, D. & Wood, R. J. Fluid-driven origami-inspired artificial muscles. *Proc. Natl Acad. Sci. USA* **114**, 13132–13137 (2017).
88. Fang, H., Li, S., Ji, H. & Wang, K. W. Dynamics of a bistable Miura-origami structure. *Phys. Rev. E* **95**, 052211 (2017).
89. McClintock, H., Temel, F. Z., Doshi, N., Koh, J. & Wood, R. J. The milliDelta: a high-bandwidth, high-precision, millimeter-scale delta robot. *Sci. Robot.* **3**, eaar3018 (2018).
90. Wang, C., Guo, H., Liu, R. & Deng, Z. A programmable origami-inspired space deployable structure with curved surfaces. *Eng. Struct.* **256**, 113934 (2022).
91. Gabler, F., Karnaushenko, D. D., Karnaushenko, D. & Schmidt, O. G. Magnetic origami creates high performance micro devices. *Nat. Commun.* **10**, 3013 (2019).
92. Velvaluri, P. et al. Origami-inspired thin-film shape memory alloy devices. *Sci. Rep.* **11**, 10988 (2021).
93. Taghavi, M., Helps, T. & Rossiter, J. Electro-ribbon actuators and electro-origami robots. *Sci. Robot.* **3**, eaau9795 (2018).
94. Reis, P. M., López Jiménez, F. & Marthelot, J. Transforming architectures inspired by origami. *Proc. Natl Acad. Sci. USA* **112**, 12234–12235 (2015).
95. Pesenti, M., Masera, G. & Fiorito, F. Exploration of adaptive origami shading concepts through integrated dynamic simulations. *J. Archit. Eng.* **24**, 04018022 (2018).
96. Le-Thanh, L., Le-Duc, T., Ngo-Minh, H., Nguyen, Q.-H. & Nguyen-Xuan, H. Optimal design of an origami-inspired kinetic façade by balancing composite motion optimization for improving daylight performance and energy efficiency. *Energy* **219**, 119557 (2021).
97. Miranda, R., Babilio, E., Singh, N., Santos, F. & Fraternali, F. Mechanics of smart origami sunscreens with energy harvesting ability. *Mech. Res. Commun.* **105**, 103503 (2020).
98. Babilio, E., Miranda, R. & Fraternali, F. On the kinematics and actuation of dynamic sunscreens with tensegrity architecture. *Front. Mater.* **6**, 00007 (2019).
99. Attia, S. Evaluation of adaptive facades: the case study of Al Bahr towers in the UAE. *QScience Connect.* **2017**, 6 (2018).
100. Xu, Y. et al. Origami system for efficient solar driven distillation in emergency water supply. *Chem. Eng. J.* **356**, 869–876 (2019).
101. Zirbel, S. A. et al. Hanaflex: a large solar array for space applications. in *Micro- and Nanotechnology Sensors, Systems, and Applications VII* Vol. 9467, 179–187 (SPIE, 2015).
102. Klett, Y., Middendorf, P., Sobek, W., Haase, W. & Heidingsfeld, M. Potential of origami-based shell elements as next-generation envelope components. in *2017 IEEE Int. Conf. Advanced Intelligent Mechatronics* 916–920 (AIM, 2017).
103. Quaglia, C. P., Yu, N., Thrall, A. P. & Paolucci, S. Balancing energy efficiency and structural performance through multi-objective shape optimization: case study of a rapidly deployable origami-inspired shelter. *Energy Build.* **82**, 733–745 (2014).
104. Lee, T.-U. & Gattas, J. M. Geometric design and construction of structurally stabilized accordion shelters. *J. Mech. Robot.* **8**, 031009 (2016).
105. Kadic, M., Milton, G. W., van Hecke, M. & Wegener, M. 3D metamaterials. *Nat. Rev. Phys.* **1**, 198–210 (2019).
106. Bertoldi, K., Vitelli, V., Christensen, J. & Van Hecke, M. Flexible mechanical metamaterials. *Nat. Rev. Mater.* **2**, 1–11 (2017).
107. Zhang, Q., Wang, X., Cai, J. & Feng, J. Motion paths and mechanical behavior of origami-inspired tunable structures. *Mater. Today Commun.* **26**, 101872 (2021).
108. Lee, T.-U., Chen, Y., Heitzmann, M. T. & Gattas, J. M. Compliant curved-crease origami-inspired metamaterials with a programmable force-displacement response. *Mater. Des.* **207**, 109859 (2021).
109. Feng, H., Peng, R., Zang, S., Ma, J. & Chen, Y. Rigid foldability and mountain–valley crease assignments of square-twist origami pattern. *Mech. Mach. Theory* **152**, 103947 (2020).
110. Saito, K., Tsukahara, A. & Okabe, Y. Designing of self-deploying origami structures using geometrically misaligned crease patterns. *Proc. R. Soc. Math. Phys. Eng. Sci.* **472**, 20150235 (2016).
111. Zhai, Z., Wang, Y., Lin, K., Wu, L. & Jiang, H. In situ stiffness manipulation using elegant curved origami. *Sci. Adv.* **6**, eabe2000 (2020).
112. Zhai, Z., Wu, L. & Jiang, H. Mechanical metamaterials based on origami and kirigami. *Appl. Phys. Rev.* **8**, 041319 (2021).
113. Kamrava, S., Mousanezhad, D., Ebrahimi, H., Ghosh, R. & Vaziri, A. Origami-based cellular metamaterial with auxetic, bistable, and self-locking properties. *Sci. Rep.* **7**, 1–9 (2017).
114. Zhao, S., Zhang, Y., Zhang, Y., Yang, J. & Kitipornchai, S. Graphene origami-enabled auxetic metallic metamaterials: an atomistic insight. *Int. J. Mech. Sci.* **212**, 106814 (2021).
115. Fang, H., Chu, S.-C. A., Xia, Y. & Wang, K.-W. Programmable self-locking origami mechanical metamaterials. *Adv. Mater.* **30**, 1706311 (2018).
116. Pinson, M. B. et al. Self-folding origami at any energy scale. *Nat. Commun.* **8**, 15477 (2017).
117. Lee, D.-Y., Kim, J.-K., Sohn, C.-Y., Heo, J.-M. & Cho, K.-J. High-load capacity origami transformable wheel. *Sci. Robot.* **6**, eabe0201 (2021).
118. Tolman, S. S., Delimont, I. L., Howell, L. L. & Fullwood, D. T. Material selection for elastic energy absorption in origami-inspired compliant corrugations. *Smart Mater. Struct.* **23**, 094010 (2014).
119. Wen, G. et al. Stacked-origami mechanical metamaterial with tailored multistage stiffness. *Mater. Des.* **212**, 110203 (2021).
120. Ma, J., Song, J. & Chen, Y. An origami-inspired structure with graded stiffness. *Int. J. Mech. Sci.* **136**, 134–142 (2018).
121. Pratapa, P. P., Liu, K., Vasudevan, S. P. & Paulino, G. H. Reprogrammable kinematic branches in tessellated origami structures. *J. Mech. Robot.* **13**, 1–22 (2021).
122. Wang, Z. et al. Origami-based reconfigurable metamaterials for tunable chirality. *Adv. Mater.* **29**, 1700412 (2017).
123. Xu, X. et al. Origami-inspired chiral metamaterials with tunable circular dichroism through mechanically guided three-dimensional assembly. *J. Appl. Mech.* **90**, 011007 (2022).
124. Li, M. et al. Origami metawall: mechanically controlled absorption and deflection of light. *Adv. Sci.* **6**, 1901434 (2019).
125. Ji, J. C., Luo, Q. & Ye, K. Vibration control based metamaterials and origami structures: a state-of-the-art review. *Mech. Syst. Signal. Process.* **161**, 107945 (2021).
126. Fuchi, K., Diaz, A. R., Rothwell, E. J., Ouedraogo, R. O. & Tang, J. An origami tunable metamaterial. *J. Appl. Phys.* **111**, 084905 (2012).
127. Zhao, P., Zhang, K. & Deng, Z. Origami-inspired lattice for the broadband vibration attenuation by Symplectic method. *Extreme Mech. Lett.* **54**, 101771 (2022).
128. Feng, H., Ma, J., Chen, Y. & You, Z. Twist of tubular mechanical metamaterials based on waterbomb origami. *Sci. Rep.* **8**, 9522 (2018).
129. Wu, S. et al. Stretchable origami robotic arm with omnidirectional bending and twisting. *Proc. Natl Acad. Sci. USA* **118**, e2110023118 (2021).
130. Hines, L., Petersen, K., Lum, G. Z. & Sitti, M. Soft actuators for small-scale robotics. *Adv. Mater.* **29**, 1603483 (2017).
131. Jiang, Y. et al. Ultra-tunable bistable structures for universal robotic applications. *Cell Rep. Phys. Sci.* **4**, 101365 (2023).
132. Jiang, H. et al. Hierarchical control of soft manipulators towards unstructured interactions. *Int. J. Robot. Res.* **40**, 411–434 (2021).
133. Lee, J.-G. & Rodrigue, H. Origami-based vacuum pneumatic artificial muscles with large contraction ratios. *Soft Robot.* **6**, 109–117 (2019).
134. Lin, Y. et al. Controllable stiffness origami "skeletons" for lightweight and multifunctional artificial muscles. *Adv. Funct. Mater.* **30**, 2000349 (2020).
135. Johnson, M. et al. Fabricating biomedical origami: a state-of-the-art review. *Int. J. Comput. Assist. Radiol. Surg.* **12**, 2023–2032 (2017).
136. Randall, C. L., Gultepe, E. & Gracias, D. H. Self-folding devices and materials for biomedical applications. *Trends Biotechnol.* **30**, 138–146 (2012).
137. Taylor, A. J., Xu, S., Wood, B. J. & Tse, Z. T. H. Origami lesion-targeting device for CT-guided interventions. *J. Imaging* **5**, 23 (2019).
138. Taylor, A., Miller, M., Fok, M., Nilsson, K. & Tsz Ho Tse, Z. Intracardiac magnetic resonance imaging catheter with origami deployable mechanisms1. *J. Med. Devices* **10**, 020957 (2016).
139. Kim, S.-J., Lee, D.-Y., Jung, G.-P. & Cho, K.-J. An origami-inspired, self-locking robotic arm that can be folded flat. *Sci. Robot.* **3**, eaar2915 (2018).
140. Banerjee, H. et al. Origami-layer-jamming deployable surgical retractor with variable stiffness and tactile sensing. *J. Mech. Robot.* **12**, 031010 (2020).
141. Bobbert, F. S. L., Janbaz, S., van Manen, T., Li, Y. & Zadpoor, A. A. Russian doll deployable meta-implants: fusion of kirigami, origami, and multi-stability. *Mater. Des.* **191**, 108624 (2020).
142. Yang, N. et al. New network architectures with tunable mechanical properties inspired by origami. *Mater. Today Adv.* **4**, 100028 (2019).
143. Prabhakar, S., Singh, J. P., Roy, D. & Prasad, N. E. Stable 3D hierarchical scaffolds by origami approach: effect of interfacial crosslinking by nanohybrid shish-kebab assemblies. *Mater. Des.* **213**, 110353 (2022).
144. Kim, S.-H. et al. Hydrogel-laden paper scaffold system for origami-based tissue engineering. *Proc. Natl Acad. Sci. USA* **112**, 15426–15431 (2015).
145. Chauhan, M. et al. An origami-based soft robotic actuator for upper gastrointestinal endoscopic applications. *Front. Robot. AI* **8**, 664720 (2021).
146. Zhu, S. & Li, T. Hydrogenation-assisted graphene origami and its application in programmable molecular mass uptake, storage, and release. *ACS Nano* **8**, 2864–2872 (2014).
147. Suzuki, H. & Wood, R. J. Origami-inspired miniature manipulator for teleoperated microsurgery. *Nat. Mach. Intell.* **2**, 437–446 (2020).
148. Sargent, B. et al. An origami-based medical support system to mitigate flexible shaft buckling. *J. Mech. Robot.* **12**, 1–16 (2020).

149. Leong, T. G. et al. Tetherless thermobiochemically actuated microgrippers. *Proc. Natl Acad. Sci. USA* **106**, 703–708 (2009).
150. Ghosh, A. et al. Stimuli-responsive soft untethered grippers for drug delivery and robotic surgery. *Front. Mech. Eng.* **3**, 7 (2017).
151. Natori, M. C., Sakamoto, H., Katsumata, N., Yamakawa, H. & Kishimoto, N. Conceptual model study using origami for membrane space structures—a perspective of origami-based engineering. *Mech. Eng. Rev.* **2**, 14–00368 (2015).
152. Miura, K. & Pellegrino, S. *Forms and Concepts for Lightweight Structures* (Cambridge Univ. Press, 2020).
153. Miura, K. *Zeta-Core Sandwich—Its Concept and Realization* (Institute of Space and Aeronautical Science, Univ. of Tokyo, 1972).
154. Miura, K. Method of packaging and deployment of large membranes in space. *Inst. Space Astronaut. Sci. Rep.* **618**, 1–9 (1985).
155. Miura, K. Concepts of deployable space structures. *Int. J. Space Struct.* **8**, 3–16 (1993).
156. Guest, S. D. & Pellegrino, S. Inextensional wrapping of flat membranes. in *Proc. First Int. Semin. Struct. Morphol.* 203–215 (Laboratoire de Mécanique et Génie Civil, Université de Montpellier II, Groupe Recherche et Réalisation de Structures Légères pour l'Architecture, Ecole d'Architecture Languedoc Roussillon, 1992).
157. De Focatiis, D. S. A. & Guest, S. D. Deployable membranes designed from folding tree leaves. *Philos. Trans. R. Soc. Lond. Ser. Math. Phys. Eng. Sci.* **360**, 227–238 (2002).
158. Parque, V. et al. Packaging of thick membranes using a multi-spiral folding approach: flat and curved surfaces. *Adv. Space Res.* **67**, 2589–2612 (2021).
159. Wilson, L., Pellegrino, S. & Danner, R. Origami sunshield concepts for space telescopes. in *54th AIAA/ASME/ASCE/AHS/ASC Struct. Struct. Dyn. Mater. Conf*. 1594 (American Institute of Aeronautics and Astronautics, 2013).
160. Wasserthal, L. T. The open hemolymph system of Holometabola and its relation to the tracheal space. *Microsc. Anat. Invertebr.* **11**, 583–620 (1998).
161. Kersten, M., Kling, G. & Burkhardt, J. IXO telescope mirror design and its performance. in *Int. Conf. Space Opt. 2010* Vol. 10565, 769–775 (SPIE, 2019).
162. Ghassaei, A., Demaine, E. D. & Gershenfeld, N. Fast, interactive origami simulation using GPU computation. *Origami* **7**, 1151–1166 (2018).
163. Demaine, E. D., Ku, J. S. & Lang, R. J. A new file standard to represent folded structures. in *Abstr. 26th Fall Workshop Comput. Geom*. 27–28 (FWCG, 2016).
164. Hu, Y., Zhou, Y. & Liang, H. Constructing rigid-foldable generalized Miura-ori tessellations for curved surfaces. *J. Mech. Robot.* **13**, 011017 (2021).
165. Dudte, L. H., Choi, G. P. & Mahadevan, L. An additive algorithm for origami design. *Proc. Natl Acad. Sci. USA* **118**, e2019241118 (2021).
166. Dang, X. et al. Inverse design of deployable origami structures that approximate a general surface. *Int. J. Solids Struct.* **234**, 111224 (2022).
167. Ze, Q. et al. Soft robotic origami crawler. *Sci. Adv.* **8**, eabm7834 (2022).
168. Chudoba, R., van der Woerd, J., Schmerl, M. & Hegger, J. ORICRETE: modeling support for design and manufacturing of folded concrete structures. *Adv. Eng. Softw.* **72**, 119–127 (2014).
169. Fernandes, R. & Gracias, D. H. Self-folding polymeric containers for encapsulation and delivery of drugs. *Adv. Drug. Deliv. Rev.* **64**, 1579–1589 (2012).
170. Nauroze, S. A., Novelino, L. S., Tentzeris, M. M. & Paulino, G. H. Continuous-range tunable multilayer frequency-selective surfaces using origami and inkjet printing. *Proc. Natl Acad. Sci. USA* **115**, 13210–13215 (2018).
171. Sareh, P., Chermprayong, P., Emmanuelli, M., Nadeem, H. & Kovac, M. Rotorigami: a rotary origami protective system for robotic rotorcraft. *Sci. Robot.* **3**, eaah5228 (2018).
172. Fathers, R. K., Gattas, J. M. & You, Z. Quasi-static crushing of eggbox, cube, and modified cube foldcore sandwich structures. *Int. J. Mech. Sci.* **101–102**, 421–428 (2015).
173. Hanna, B. H., Lund, J. M., Lang, R. J., Magleby, S. P. & Howell, L. L. Waterbomb base: a symmetric single-vertex bistable origami mechanism. *Smart Mater. Struct.* **23**, 094009 (2014).
174. Fonseca, L. M. & Savi, M. A. Nonlinear dynamics of an autonomous robot with deformable origami wheels. *Int. J. Non-Linear Mech.* **125**, 103533 (2020).
175. Kuribayashi, K. et al. Self-deployable origami stent grafts as a biomedical application of Ni-rich TiNi shape memory alloy foil. *Mater. Sci. Eng. A* **419**, 131–137 (2006).
176. Yasuda, H., Chong, C., Charalampidis, E. G., Kevrekidis, P. G. & Yang, J. Formation of rarefaction waves in origami-based metamaterials. *Phys. Rev. E* **93**, 043004 (2016).
177. Evans, T. A., Lang, R. J., Magleby, S. P. & Howell, L. L. Rigidly foldable origami gadgets and tessellations. *R. Soc. Open. Sci.* **2**, 150067 (2015).
178. Lang, R. J., Magleby, S. & Howell, L. Single degree-of-freedom rigidly foldable cut origami flashers. *J. Mech. Robot.* **8**, 031005 (2016).
179. Chen, Z. et al. Ron Resch origami pattern inspired energy absorption structures. *J. Appl. Mech.* **86**, 011005 (2018).
180. Overvelde, J. T. B., Weaver, J. C., Hoberman, C. & Bertoldi, K. Rational design of reconfigurable prismatic architected materials. *Nature* **541**, 347–352 (2017).
181. Babaee, S., Overvelde, J. T. B., Chen, E. R., Tournat, V. & Bertoldi, K. Reconfigurable origami-inspired acoustic waveguides. *Sci. Adv.* **2**, e1601019 (2016).

Acknowledgements

D.M. acknowledges financial support from the European Union project ERC-CoG 2022-SFOAM-101086644. K.L. is supported by the National Key Research and Development Program of China (grant 2022YFB4701900) and the National Natural Science Foundation of China (grant 12372159). P.P.P. acknowledges support from the Indian Institute of Technology Madras through the seed grant and the Science & Engineering Research Board (SERB) of the Department of Science & Technology, Government of India (award SRG/2019/000999). Y.C. acknowledges the support of the National Natural Science Foundation of China (Projects 52320105005, 52035008) and the New Cornerstone Science Foundation through the XPLORER PRIZE (XPLORER-2020-1035). G.H.P. acknowledges financial support from the Natural Science Foundation (NSF) project 2323276. C.D. acknowledges the Army Research Office under Cooperative Agreement Number W911NF-22-2-0109.

Author contributions

The authors contributed equally to all aspects of the article.

Competing interests

The authors declare no competing interests.

Additional information

Peer review information *Nature Reviews Methods Primers* thanks James McInerney, Jianguo Cai and the other, anonymous, reviewer(s) for their contribution to the peer review of this work.

Related links

GIMP: https://www.gimp.org/
ImageJ: https://imagej.nih.gov/ij/index.html
nanoCad: https://nanocad.com/products/nanocad-free/
Quick Time: https://support.apple.com/downloads/quicktime
Starshade origami: https://www.jpl.nasa.gov/edu/learn/project/space-origami-make-your-own-starshade/
VLC: https://www.videolan.org/vlc/